J Gastroenterol (2010) 45:1247–1254
DOI 10.1007/s00535-010-0272-y

Absence of invariant natural killer T cells deteriorates liver inflammation and fibrosis in mice fed high-fat diet

Takuya Miyagi · Tetsuo Takehara · Akio Uemura · Kumiko Nishio · Satoshi Shimizu · Takahiro Kodama · Hayato Hikita · Wei Li · Akira Sasakawa · Tomohide Tatsumi · Kazuyoshi Ohkawa · Tatsuya Kanto · Naoki Hiramatsu · Norio Hayashi

Received: 28 November 2009 / Accepted: 31 May 2010 / Published online: 2 July 2010

Abstract
Background Invariant natural killer T (iNKT) cells have been suggested to play critical roles in a wide range of immune responses by acting in a proinflammatory or anti-inflammatory manner. Nonalcoholic steatohepatitis (NASH) is a chronic liver disease progressing to advanced cirrhosis and hepatocellular carcinoma. Despite the abundance of iNKT cells in the liver, their role in the pathogenesis of NASH remains obscure. Here, we investigated their role in the development of diet-induced steatosis/steatohepatitis.
Methods We used BALB/c wild-type mice and Jα18-deficient (KO) mice lacking iNKT cells fed either a normal diet or a high-fat diet (HFD). The liver and blood were collected from these mice to examine liver inflammation, steatosis, and fibrosis at the indicated time points.
Results KO mice fed the HFD, compared with control mice fed the HFD, exhibited a clearly higher serum alanine aminotransferase level and a greater number of hepatic inflammatory foci, although there was no significant difference in hepatic lipid retention between these groups of mice. The HFD enhanced hepatic messenger RNA expression of inflammatory cytokines and chemokines in KO but not in control mice. The HFD also increased the proportion of hepatic CD4 T cells and CD8 T cells that composed hepatic inflammatory foci in KO mice, but not in the controls. Prolonged feeding with the HFD augmented liver fibrosis in KO but not in control mice.
Conclusions These findings indicate that iNKT cells play a protective role against liver inflammation progressing to fibrosis, but not against steatosis, enhanced by dietary excess fat, suggesting a key role of these cells in NASH pathogenesis.

Keywords iNKT cells · Nonalcoholic fatty liver disease · Nonalcoholic steatohepatitis · Cytokine · Chemokine

Abbreviations

NAFLD	Nonalcoholic fatty liver disease
NASH	Nonalcoholic steatohepatitis
iNKT	Invariant natural killer T
NK	Natural killer
TCR	T cell receptor
Th	T helper
IFN	Interferon
IL	Interleukin
WT	Wild type
ND	Normal diet
HFD	High-fat diet
KO	Jα18-deficient
ALT	Alanine aminotransferase
RT-PCR	Reverse transcription polymerase chain reaction
H&E	Hematoxylin–eosin
SEM	Standard error of the mean
TNF	Tumor necrosis factor
CCL	Chemokine (C–C motif) ligand
CXCL	Chemokine (C–X–C motif) ligand

T. Miyagi · T. Takehara · A. Uemura · K. Nishio · S. Shimizu · T. Kodama · H. Hikita · W. Li · A. Sasakawa · T. Tatsumi · K. Ohkawa · T. Kanto · N. Hiramatsu · N. Hayashi (✉)
Department of Gastroenterology and Hepatology, Osaka University Graduate School of Medicine, 2-2 Yamada-oka, Suita, Osaka 565-0871, Japan
e-mail: hayashin@gh.med.osaka-u.ac.jp

Introduction

Nonalcoholic fatty liver disease (NAFLD) is a spectrum of liver disorders ranging from nonalcoholic steatosis to nonalcoholic steatohepatitis (NASH), which can develop to progressive disease including advanced liver fibrosis and hepatocellular carcinoma [1, 2]. Prolonged overnutrition causes accumulation of free fatty acid and triglycerides within the liver, which is referred to as steatosis. Simple steatosis leads to a predisposition for steatohepatitis, which exhibits inflammatory cell accumulation and fibrosis in the liver in addition to the steatosis [1, 2]. To transform from steatosis to steatohepatitis, several key biological responses such as oxidative stress, mitochondrial dysfunction, endoplasmic reticulum stress, and abnormal cytokine properties have been reported to be required [1–4]. However, the immunological aspect, in particular, that is involved in the development of steatosis/steatohepatitis remains to be fully elucidated.

Invariant natural killer T (iNKT) cells are characterized by the expression of surface markers of natural killer (NK) cells together with a single invariant T cell receptor (TCR) encoded by Vα14-Jα18 in mice and Vα24-Jα18 in humans [5]. These cells are included within the population of T cells expressing NK cell markers, also known as NKT cells [5, 6]. iNKT cells recognize glycolipid antigens presented in association with the major histocompatibility complex class Ib molecule CD1d [5], which is expressed on a variety of cells including dendritic cells, B cells, and stellate cells, as well as hepatocytes in the liver [5, 7, 8]. Following the recognition of antigens via TCR, iNKT cells have the ability to produce the T-helper (Th) 1 cytokine, interferon (IFN)-γ, and the Th2 cytokines, interleukin (IL)-4, -5, and -13, modulating subsequent immune responses [5, 6, 9]. These cells have been shown to play a proinflammatory role in some immune responses and an anti-inflammatory role in other immune responses [5, 6, 9]. iNKT cells most frequently reside in the liver in mice [10, 11]. Although humans appear to have proportionally fewer iNKT cells than mice, human iNKT cells also preferentially reside in the liver [12, 13]. Several lines of evidence indicate that the number of NKT cells is dysregulated in the development of NAFLD. Hepatic iNKT cells or NK1.1+ CD3+/TCRβ+ NKT cells, for instance, have been reported to decrease with the development of steatosis in wild-type (WT) as well as leptin-deficient ob/ob mice [14–17]. A reduced level of peripheral Vα24+ NKT cells has been associated with human NAFLD [18]. On the other hand, CD56+ CD3+ NKT cells have been recently reported to be increased in the livers of patients with NAFLD [19]. Also, the adoptive transfer of NK1.1+ CD3+ NKT cells has been shown to alleviate hepatic steatosis in ob/ob mice [20]. However, the precise role of NKT cells in the pathogenesis of NAFLD has not been investigated in the presence of a deficiency of these cells.

In the present study, we used iNKT cell-deficient as well as WT mice fed either a normal diet (ND) or a high-fat diet (HFD), and examined the role of these cells in the development of HFD-induced steatosis/steatohepatitis. We found that the lack of iNKT cells, together with the HFD, led to liver inflammation, which was characterized by the enhanced gene expression of inflammatory cytokines and chemokines and by T cell accumulation. We also found that prolonged liver inflammation in the absence of iNKT cells developed to liver fibrosis which was strongly enhanced by the HFD. This study delineated an immunoregulatory function of iNKT cells and their key role against liver inflammation progressing to fibrosis exacerbated by an HFD, which might represent a clinical aspect of human progressive NAFLD.

Materials and methods

Animals and animal care

Specific pathogen-free BALB/c WT mice were purchased from CLEA Japan (Tokyo, Japan) as needed. Breeding pairs of BALB/c Jα18-deficient (KO) mice [21, 22] were provided by Drs. Masaru Taniguchi and Ken-ichiro Seino (RIKEN, Yokohama, Japan). The KO mice were confirmed to have no iNKT cells by the use of mouse-CD1d tetramers loaded with α-galactosylceramide in the flow cytometry procedure described below (data not shown). These mice were kept in isolation facilities at the Institute of Experimental Animal Science, Osaka University. They were housed in groups of five in filter cages and were maintained in a temperature-controlled, specific-pathogen-free room on 12-h light and dark cycles with ad libitum access to water and diet as indicated.

Experimental protocol

Male mice used in the experiments were fed an irradiated HFD consisting of 56.7% of the calories from fat (HFD32; CLEA Japan) or an irradiated ND consisting of 14% of the calories from fat (CRF-1; Oriental Yeast, Osaka, Japan), starting from when the mice were 6–8 weeks old. In preliminary experiments, we monitored the body weight of the WT mice and KO mice fed the ND or HFD every 2 weeks after the initiation of feeding, because a gain of body weight usually parallels the level of hepatic steatosis as well as obesity. We did not observe a gain of body weight of more than 25% until 4 weeks after the initiation of feeding. In mice fed the HFD, the body weight gain reached a plateau around 14–16 weeks after the initiation

of feeding. These observations led us to set the time point for estimating liver steatosis and injury and inflammation or liver fibrosis during the course of feeding at week 5 or week 15, respectively. At the end of the indicated periods, the mice were weighed and anesthetized with pentobarbital sodium, and then their abdomens were opened. Following blood sampling via the inferior caval vein, the portal vein and inferior caval vein were cut to enable blood outflow and then the liver was removed, weighed, and processed for further analyses. All animal experimental protocols were approved by the Institute of Experimental Animal Science, Osaka University. To evaluate the levels of liver injury, serum alanine aminotransferase (ALT) activities were measured as previously described [23]. To determine the levels of steatosis, total lipids were extracted from the liver and then triglyceride content was measured as previously described [24].

Flow cytometric analysis

Liver mononuclear cell populations were prepared as previously described [11, 23]. Cell surface staining of the prepared cells was performed as described [11, 23], using the following antibodies or tetramers: fluorescein isothiocyanate-conjugated anti-CD49b (DX5), phycoerythrin-conjugated anti-CD4 (H129.19), peridinin chlorophyll protein-conjugated anti-CD8α (53-6.7), and allophycocyanin-conjugated anti-TCRβ (H57-597) monoclonal antibody, or fluorescein isothiocyanate-conjugated anti-TCRβ, phycoerythrin-conjugated anti-CD4, peridinin chlorophyll protein-conjugated anti-CD45R/B220 (RA3-6B2) monoclonal antibody, and allophycocyanin-conjugated mouse-CD1d tetramers loaded with α-galactosylceramide. All antibodies were purchased from BD Biosciences (San Jose, CA, USA). Mouse CD1d tetramer was obtained from Proimmune (Oxford, UK) and the loading with α-galactosylceramide was performed following the manufacturer's protocol. The stained cells were analyzed with a FACScan (Becton Dickinson, Mountain View, CA, USA), and the data were processed using the CELLQuest program (Becton Dickinson). iNKT cells were detected on electronically gated CD45R/B220- TCRβ+ CD1d-tetramer-reactive cells.

RNA isolation and analysis

Total RNA was isolated from frozen liver tissues by using an RNeasy kit (QIAGEN, Hilden, Germany) following the manufacturer's protocol. Complementary DNA was synthesized from isolated RNA using SuperScript III and random hexamer (Invitrogen, Carlsbad, CA, USA). Real-time reverse transcription polymerase chain reaction (RT-PCR) analysis was performed using TaqMan Gene Expression Assays (Applied Biosystems, Foster City, CA, USA) normalized to beta-actin.

Histological evaluation

The removed liver was partly fixed in 10% formalin for staining with hematoxylin–eosin (H&E), Sirius-Red, or Oil-red-O, or it was immediately embedded in Tissue-Tek OCT compound (Sakura Finetechnical, Tokyo, Japan) and frozen in liquid nitrogen for immunohistochemical staining. Sirius-Red staining was performed to assess liver fibrosis, which was quantified by the extent of the area, using image-analysis software, WinROOF (Mitani, Fukui, Japan). Intracellular lipid was stained with Oil-red-O. To evaluate the infiltration of CD4+ cells or CD8+ cells into the liver, acetone-fixed fresh-frozen tissue sections were immunostained with anti-mouse CD4 (H129.19) or anti-mouse CD8α (53-6.7) monoclonal antibody, respectively, using a VECTASTAIN ABC kit (Vector Laboratories, Burlingame, CA, USA) following the manufacturer's protocol. The sections were developed with diaminobenzidine (DAB) substrate (Vector Laboratories) and then counter-stained with hematoxylin. Antibody against CD4 or CD8 was purchased from BD Biosciences.

Statistical analysis

The statistical significance of differences between two groups was determined by applying the Mann–Whitney *U*-test. Statistical significance was defined as $P < 0.05$. All data are shown as mean ± standard error of the mean (SEM).

Results

Lipid accumulation in the liver induced by the HFD was independent of the presence or absence of iNKT cells

To investigate the role of iNKT cells in the development of diet-induced steatosis/steatohepatitis, we fed the ND or HFD to WT and KO mice for 5 weeks. The HFD increased the body weight by around 30% at week 5 in both WT and KO mice, while the ND increased it by around 14% (HFD-fed WT mice 31.6 ± 2.4%, HFD-fed KO mice 29.7 ± 5.6%, ND-fed WT mice 15.5 ± 0.6%, ND-fed KO mice 13.5 ± 1.1%; $n = 5$). The weight gains with the HFD or ND were not significantly different between WT and KO mice. Evaluation of the liver weight at week 5 showed that the HFD-fed WT or KO mice possessed significantly heavier livers than the ND-fed WT or KO mice, respectively, without any significant differences between the WT and KO mice (HFD-fed WT mice 1.95 ± 0.06 g, HFD-fed

KO mice 1.89 ± 0.07 g, ND-fed WT mice 1.52 ± 0.04 g, ND-fed KO mice 1.50 ± 0.06 g; $n = 5$).

We next performed Oil-red-O staining of liver sections from the mice to examine whether the absence of iNKT cells would affect the HFD-induced lipid accumulation in the liver. The staining showed that the HFD, compared with the ND, induced marked lipid retention in hepatocytes in both WT and KO mice (Fig. 1a). Evaluation of the liver triglyceride level demonstrated that the HFD, compared with the ND, clearly induced triglyceride accumulation in the livers of both WT and KO mice, without a significant difference between these groups of mice (Fig. 1b).

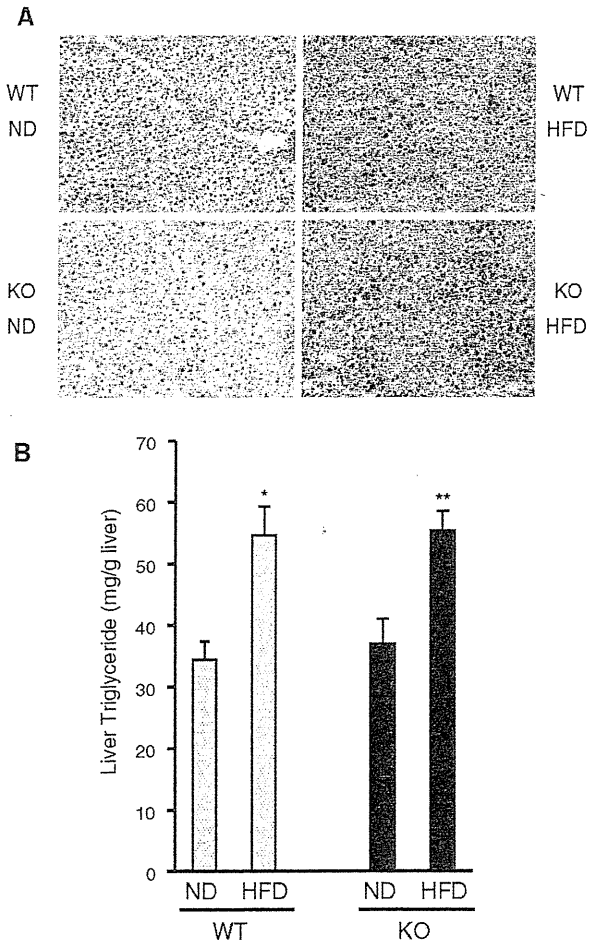

Fig. 1 Lipid accumulation in the liver induced by high-fat diet (*HFD*). Livers were obtained from BALB/c wild-type (*WT*) and BALB/c Jα18-deficient (*KO*) mice fed either a normal diet (*ND*) or an HFD for 5 weeks. **a** Lipid accumulation in liver sections was visualized by Oil-red-O staining. Representative images are shown (×200). **b** Hepatic triglyceride levels were quantified. Data shown are means ± SEM from five mice in each group. Data are representative of more than four independent experiments. $*P < 0.05$ versus WT fed ND. $**P < 0.05$ versus KO fed ND

Collectively, these results suggested that the absence of iNKT cells did not affect the level of HFD-induced steatosis.

HFD augmented liver injury and inflammation in the absence of iNKT cells

To examine the levels of liver injury, we measured ALT activity in serum from WT and KO mice fed the ND or HFD at week 5 after the start of being fed the diets. The serum ALT level in the HFD-fed WT mice (35.8 ± 1.98 IU/l) was significantly higher than that in the ND-fed WT mice (25.2 ± 0.66 IU/l) (Fig. 2a). The serum ALT level in the HFD-fed KO mice (174.8 ± 61.2 IU/l) was also significantly higher than that in the ND-fed KO mice (36.4 ± 7.48 IU/l). It was also higher than that in the HFD-fed KO mice at week 2 (83.3 ± 16.5 IU/l). Of note is the finding that the magnitude of the increase in ALT level at week 5 was clearly much higher in KO (4.9-fold) than in

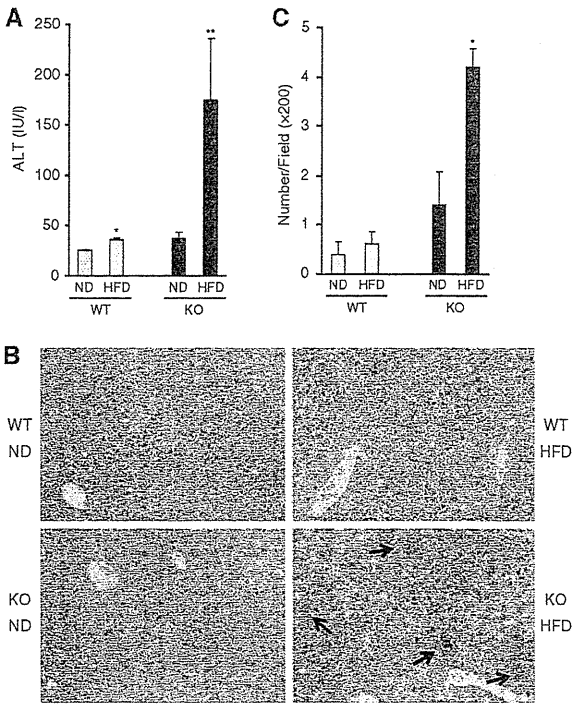

Fig. 2 Liver injury and inflammation exacerbated by HFD in the absence of invariant natural killer T (*iNKT*) cells. Serum and livers were obtained from wild-type (*WT*) and Jα18-deficient (*KO*) mice fed either a normal diet (*ND*) or a high-fat diet (*HFD*) for 5 weeks. **a** Serum alanine aminotransferase (*ALT*) levels were measured. $*P < 0.05$ versus WT fed ND. $**P < 0.05$ versus KO fed ND. **b** Liver tissues were stained with hematoxylin–eosin. Representative images are shown (×200). *Arrows* indicate the inflammatory foci. **c** The numbers of the foci were counted in five different fields per section. $*P < 0.05$ versus KO fed ND. All data shown are means ± SEM from five mice in each group. Data are representative of more than four independent experiments

WT mice (1.5-fold), even though the serum ALT level in the ND-fed KO mice was modestly higher than that in the ND-fed WT mice.

We next conducted histological analyses of liver sections from the mice. H&E staining revealed that the livers from KO mice fed the HFD possessed not only steatotic areas but also scattered inflammatory foci composed of gathering nonparenchymal cells (Fig. 2b). Although inflammatory foci were also observed in the livers from KO mice fed the ND, a larger number of foci could clearly be seen in KO mice fed the HFD than in KO mice fed the ND (Fig. 2c). In contrast, WT mice fed the HFD, as well as those given the ND, showed few inflammatory foci. Taken together, these results indicated that the HFD augmented liver inflammation in KO mice but not in WT mice.

The HFD enhanced hepatic inflammation-related gene expression in the absence of iNKT cells

To understand the underlying mechanisms of the hepatic inflammation induced by the HFD in the absence of iNKT cells, we first examined the levels of several cytokines and chemokines in the livers from mice at week 5 after they had been started on the diets. Real-time RT-PCR analyses revealed that the messenger RNA expression of tumor necrosis factor (TNF)-α, IFN-γ, IL-10, chemokine (C–C motif) ligand (CCL) 2 and 4, and chemokine (C–X–C motif) ligand (CXCL) 9 and 10 were remarkably upregulated by the HFD, compared with the ND, in KO but not in WT mice (Fig. 3), although these values in KO mice fed the ND were modestly higher than those in WT mice fed the ND. In contrast, the messenger RNA expression of IL-4, -5, and -13 did not show any detectable levels in the livers from both WT and KO mice fed either the ND or HFD.

The HFD altered the proportions of subpopulations in liver mononuclear cells from KO mice, but not in those from WT mice

We next examined the phenotype of mononuclear cells in livers from mice at week 5 of feeding. Flow cytometric analyses demonstrated that the proportion of CD4+ TCRβ+ CD4 T cells was lower in KO mice fed the ND than in WT mice fed the ND (Fig. 4a), which might have resulted from a lack of iNKT cells partly composed of CD4+ cells [5]. The proportion of CD49b+ TCRβ− NK cells or CD8+ TCRβ+ CD8 T cells was higher in KO mice fed the ND than in WT mice fed the ND. The HFD did not lead to any significant changes in the proportion of hepatic CD4 T, CD8 T, NK, or iNKT cells in WT mice. In contrast, the HFD induced significant increases in the proportion of hepatic CD4 T cells and CD8 T cells, but not of NK cells, in KO mice. We then examined the distribution of these cells

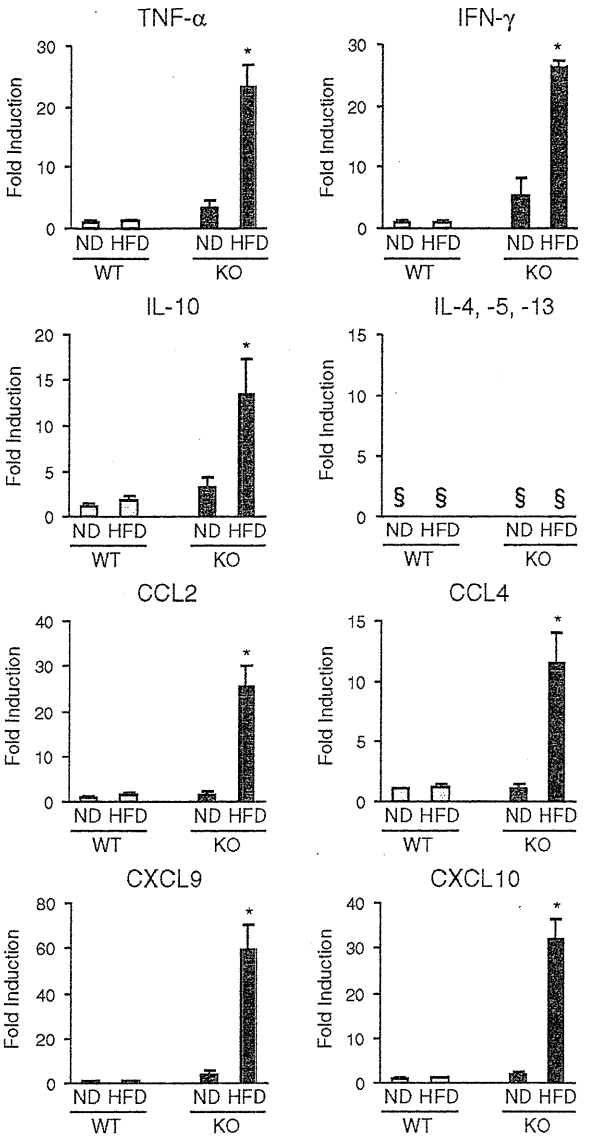

Fig. 3 Inflammatory cytokine and chemokine gene expression in the liver. Liver tissues were obtained from wild-type (*WT*) and Jα18-deficient (*KO*) mice fed either a normal diet (*ND*) or a high-fat diet (*HFD*) for 5 weeks. Liver RNA levels of the indicated genes and beta-actin as a control were analyzed using real-time reverse transcription polymerase chain reaction (RT-PCR). Data are shown as the fold increase of HFD-fed WT, ND-fed KO, or HFD-fed KO compared with ND-fed WT mice, with means ± SEM from five mice in each group. Data are representative of more than four independent experiments. *TNF-α* Tumor necrosis factor alpha, *IFN-γ* interferon gamma, *IL* interleukin, *CCL* chemokine (C–C motif) ligand, *CXCL* chemokine (C–X–C motif) ligand. §, not detected. *$P < 0.05$ versus KO fed ND

in the liver. Immunohistochemical examination revealed that CD4+ cells and CD8+ cells formed foci surrounding hepatocytes in the livers of KO mice (Fig. 4b), which partly corresponded to the inflammatory foci observed in the

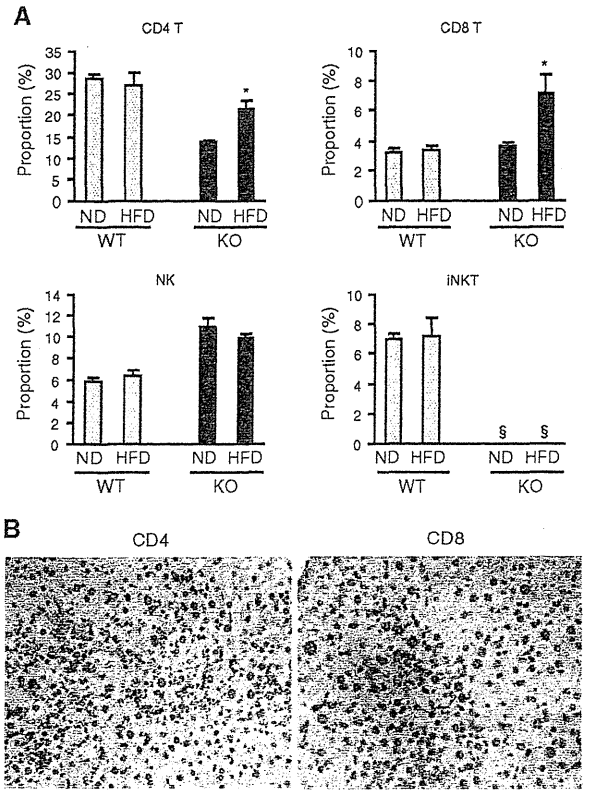

Fig. 4 Involvement of CD4 T and/or CD8 T cells in liver inflammation. Livers were obtained from wild-type (*WT*) and Jα18-deficient (*KO*) mice fed either a normal diet (*ND*) or a high-fat diet (*HFD*) for 5 weeks. **a** Prepared mononuclear cells from the livers were stained with cell markers indicated in "Materials and methods". Proportions of the indicated cell population were analyzed by flow cytometry. Data shown are means ± SEM from five mice in each group. Data are representative of more than four independent experiments. §, not detected. $*P < 0.05$ versus KO fed ND. **b** Liver sections were analyzed by immunohistochemical staining for CD4- or CD8-positive cells. Representative images are shown (×200)

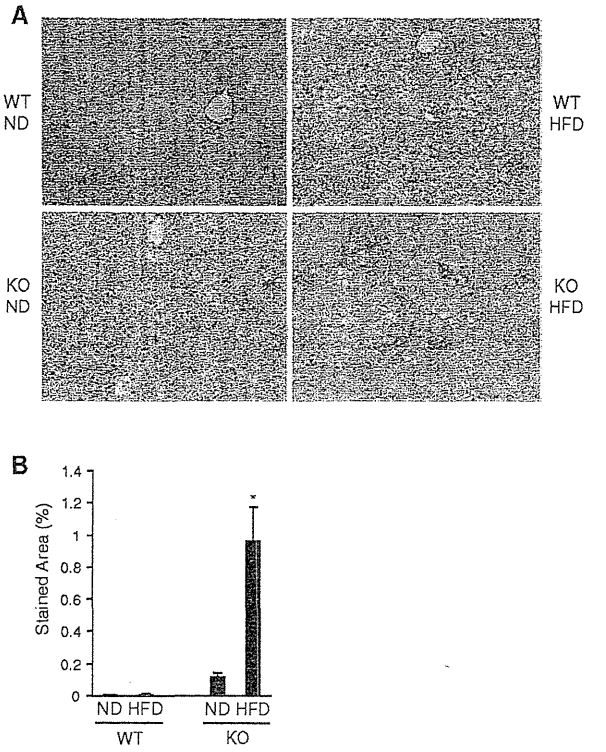

Fig. 5 Liver fibrosis following inflammation in the absence of iNKT cells. Livers were obtained from wild-type (*WT*) and Jα18-deficient (*KO*) mice fed either a normal diet (*ND*) or a high-fat diet (*HFD*) for 15 weeks. **a** Liver tissues were stained with Sirius-Red to assess liver fibrosis. Representative images are shown (×200). **b** The stained areas were evaluated in five different fields per section. Data shown are means ± SEM from five mice in each group. Data are representative of more than two independent experiments. $*P < 0.05$ versus KO fed ND

H&E-stained liver sections of KO mice. WT mice fed either the ND or HFD did not display such foci consisting of stained cells in the livers. Collectively, these results suggested that CD4 T and/or CD8 T cells played a role in the HFD-enhanced liver inflammation in KO mice.

The HFD led to the development of liver fibrosis in the absence of iNKT cells

Persistent hepatic inflammation causes fibrotic changes in the liver [25]. To investigate whether inflammation with steatosis due to the HFD in KO mice would induce fibrosis in the liver, we fed the ND or HFD to WT and KO mice for a longer period of 15 weeks. H&E staining and Oil-red-O staining showed that KO mice fed the HFD possessed the inflammatory foci, together with lipid retention in the liver, at week 15, as well as showing these findings at week 5, and that WT mice fed the HFD showed lipid retention, but few inflammatory foci, in the liver at week 15 (data not shown). Sirius-Red staining revealed clear fibrosis in the livers from KO mice fed the HFD and also in the livers from KO mice fed the ND, but to a much lesser extent (Fig. 5a). In contrast, the staining showed no obvious fibrosis in the livers from WT mice fed the HFD or in those given the ND. Quantitative analyses to evaluate the stained areas also showed that the HFD-fed KO mice possessed significantly greater areas of hepatic fibrosis than the ND-fed KO mice, while WT mice fed either the ND or HFD had few fibrotic areas (Fig. 5b). Taken together, these results indicated that the HFD led to the development of liver fibrosis accompanied by steatohepatitis in KO mice.

Discussion

An increasing amount of evidence suggests that iNKT cells play a role in immune responses in the liver [12], although

the exact implication of that role is controversial. iNKT cells, for instance, have been reported to play a critical role in animal models of liver injury induced by concanavalin A, α-galactosylceramide, or salmonella infection [26–28], suggesting a proinflammatory role of these cells. On the other hand, iNKT cells have been very recently implicated in the suppression of liver damage in a mouse model of cholestasis [29], suggesting an anti-inflammatory role of these cells. The present study, using iNKT cell-deficient mice fed an HFD, demonstrated that the HFD led to the development of steatohepatitis with fibrosis in the absence of iNKT cells, while the HFD led to steatosis but not steatohepatitis in the presence of these cells. This suggests that iNKT cells play a critical role in suppressing the development of inflammation and fibrosis in the steatotic liver.

Our real-time RT-PCR analyses demonstrated that CCL2, CCL4, CXCL9, and CXCL10 were remarkably upregulated by the HFD in KO mice but not in WT mice (Fig. 3). CCL2 or CCL4 has the ability to attract predominantly Th1 cells via chemokine (C–C motif) receptor 2 or 5, respectively. CXCL9 and CXCL10 also attract predominantly Th1 cells via chemokine (C–X–C motif) receptor 3 [30, 31]. Indeed, Th1 cytokines such as TNF-α and IFN-γ were remarkably upregulated by the HFD in KO mice but not in WT mice. Although IL-10, which is one of the anti-inflammatory cytokines, was also upregulated by the HFD in KO mice but not in WT mice, the upregulation of IL-10 may have counteracted the upregulation of the proinflammatory Th1 cytokines TNF-α and IFN-γ. Our flow cytometric analyses and immunohistochemical analyses showed that the proportions of CD4 T and CD8 T cells were increased (Fig. 4a) and that these cells also accumulated to form foci (Fig. 4b) in the livers of KO mice fed the HFD. Bigorgne et al. [32] reported that HFD-induced obesity in leptin-deficient ob/ob mice rendered hepatic mononuclear cells, particularly CD4 T and CD8 T cells, sensitive to chemokines such as CXCL12 and CXCL13, which attract T cells, suggesting an important role of chemokines in liver inflammation with steatosis. Although the sources of the chemokines upregulated in our model were not clear, these chemokines presumably play an important role in the infiltration of proinflammatory cells in the liver of the KO mice fed the HFD. iNKT cells suppress the production of these chemokines directly or indirectly; thus, they may prevent steatohepatitis induced by an HFD.

The liver can be anatomically exposed to gut-derived contents, such as food antigens and bacterial products, via the portal vein [33, 34]. Once these entities flow into the liver, they can activate a variety of cells in the liver, which may be associated with certain types of liver disease [33, 34]. Gut-derived food-antigens can activate T cells [33] and gut-derived bacterial products can stimulate all resident cells in the liver, such as hepatocytes, Kupffer cells, stellate cells, and dendritic cells, via toll-like receptors [33–36]. Moreover, fat itself, particularly saturated fatty acids, stimulates an immune response in the liver [37, 38]. On the other hand, the liver is an immune-tolerogenic organ, in which immune-suppressive cells may play a critical role to keep this organ immunologically silent [33]. The present study demonstrated that liver inflammation was greatly exacerbated—where CD4 T and/or CD8 T cells infiltrated to form foci surrounding damaged hepatocytes—by an HFD in the absence of iNKT cells. This suggests a suppressive role of iNKT cells in the development of liver inflammation with steatosis. Thus, iNKT cells may play an important role in keeping the liver immunologically silent, and the absence of iNKT cells together with steatosis may elicit a break of hepatic immune tolerance, resulting in the activation of CD4 T and/or CD8 T cells to provoke liver inflammation. Consistent with this speculation is the observation that the absence of iNKT cells, even without steatosis, caused modest liver inflammation.

In conclusion, iNKT cells suppress liver inflammation progressing to fibrosis that is exacerbated by HFD-induced steatosis, thus contributing to the maintenance of immune homeostasis in the liver. This study has shed some light on iNKT cells as immunoregulatory cells and their key role in the pathogenesis of NAFLD.

Acknowledgments The authors thank Drs. Masaru Taniguchi and Ken-ichiro Seino for providing Jα18-deficient BALB/c mice. This work was supported by a Grant-in-Aid for Scientific Research (to T. Takehara) and Global Centers of Excellence Program (to T. Miyagi) from the Ministry of Education, Culture, Sports, Science and Technology of Japan.

References

1. Angulo P. Nonalcoholic fatty liver disease. N Engl J Med. 2002;346:1221–31.
2. Clark JM, Brancati FL, Diehl AM. Nonalcoholic fatty liver disease. Gastroenterology. 2002;122:1649–57.
3. Maher JJ, Leon P, Ryan JC. Beyond insulin resistance: Innate immunity in nonalcoholic steatohepatitis. Hepatology. 2008;48:670–8.
4. Tilg H, Diehl AM. Cytokines in alcoholic and nonalcoholic steatohepatitis. N Engl J Med. 2000;343:1467–76.
5. Bendelac A, Savage PB, Teyton L. The biology of NKT cells. Annu Rev Immunol. 2007;25:297–336.
6. Godfrey DI, Kronenberg M. Going both ways: immune regulation via CD1d-dependent NKT cells. J Clin Invest. 2004;114:1379–88.
7. Trobonjaca Z, Leithäuser F, Möller P, Schirmbeck R, Reimann J. Activating immunity in the liver. I. Liver dendritic cells (but not hepatocytes) are potent activators of IFN-gamma release by liver NKT cells. J Immunol. 2001;167:1413–22.
8. Winau F, Hegasy G, Weiskirchen R, Weber S, Cassan C, Sieling PA, et al. Ito cells are liver-resident antigen-presenting cells for activating T cell responses. Immunity. 2007;26:117–29.

9. Matsuda JL, Mallevaey T, Scott-Browne J, Gapin L. CD1d-restricted iNKT cells, the 'Swiss-Army knife' of the immune system. Curr Opin Immunol. 2008;20:358–68.
10. Matsuda JL, Naidenko OV, Gapin L, Nakayama T, Taniguchi M, Wang CR, et al. Tracking the response of natural killer T cells to a glycolipid antigen using CD1d tetramers. J Exp Med. 2000;192:741–54.
11. Miyagi T, Takehara T, Tatsumi T, Kanto T, Suzuki T, Jinushi M, et al. CD1d-mediated stimulation of natural killer T cells selectively activates hepatic natural killer cells to eliminate experimentally disseminated hepatoma cells in murine liver. Int J Cancer. 2003;106:81–9.
12. Exley MA, Koziel MJ. To be or not to be NKT: natural killer T cells in the liver. Hepatology. 2004;40:1033–40.
13. Norris S, Doherty DG, Collins C, McEntee G, Traynor O, Hegarty JE, et al. Natural T cells in the human liver: cytotoxic lymphocytes with dual T cell and natural killer cell phenotype and function are phenotypically heterogenous and include Valpha24-JalphaQ and gammadelta T cell receptor bearing cells. Hum Immunol. 1999;60:20–31.
14. Guebre-Xabier M, Yang S, Lin HZ, Schwenk R, Krzych U, Diehl AM. Altered hepatic lymphocyte subpopulations in obesity-related murine fatty livers: potential mechanism for sensitization to liver damage. Hepatology. 2000;31:633–40.
15. Li ZP, Soloski MJ, Diehl AM. Dietary factors alter hepatic innate immune system in mice with nonalcoholic fatty liver disease. Hepatology. 2005;42:880–5.
16. Ma X, Hua J, Li Z. Probiotics improve high fat diet-induced hepatic steatosis and insulin resistance by increasing hepatic NKT cells. J Hepatol. 2008;49:821–30.
17. Miyazaki Y, Iwabuchi K, Iwata D, Miyazaki A, Kon Y, Niino M, et al. Effect of high fat diet on NKT cell function and NKT cell-mediated regulation of Th1 responses. Scand J Immunol. 2008;67:230–7.
18. Xu CF, Yu CH, Li YM, Xu L, Du J, Shen Z. Association of the frequency of peripheral natural killer T cells with nonalcoholic fatty liver disease. World J Gastroenterol. 2007;13:4504–8.
19. Tajiri K, Shimizu Y, Tsuneyama K, Sugiyama T. Role of liver-infiltrating CD3+ CD56+ natural killer T cells in the pathogenesis of nonalcoholic fatty liver disease. Eur J Gastroenterol Hepatol. 2009;21:673–80.
20. Elinav E, Pappo O, Sklair-Levy M, Margalit M, Shibolet O, Gomori M, et al. Adoptive transfer of regulatory NKT lymphocytes ameliorates non-alcoholic steatohepatitis and glucose intolerance in ob/ob mice and is associated with intrahepatic CD8 trapping. J Pathol. 2006;209:121–8.
21. Cui J, Shin T, Kawano T, Sato H, Kondo E, Toura I, et al. Requirement for Valpha14 NKT cells in IL-12-mediated rejection of tumors. Science. 1997;278:1623–6.
22. Harada M, Magara-Koyanagi K, Watarai H, Nagata Y, Ishii Y, Kojo S, et al. IL-21-induced Bepsilon cell apoptosis mediated by natural killer T cells suppresses IgE responses. J Exp Med. 2006;203:2929–37.
23. Miyagi T, Takehara T, Tatsumi T, Suzuki T, Jinushi M, Kanazawa Y, et al. Concanavalin A injection activates intrahepatic innate immune cells to provoke an antitumor effect in murine liver. Hepatology. 2004;40:1190–6.
24. Kamada Y, Matsumoto H, Tamura S, Fukushima J, Kiso S, Fukui K, et al. Hypoadiponectinemia accelerates hepatic tumor formation in a nonalcoholic steatohepatitis mouse model. J Hepatol. 2007;47:556–64.
25. Friedman SL. Mechanisms of hepatic fibrogenesis. Gastroenterology. 2008;134:1655–69.
26. Ishigami M, Nishimura H, Naiki Y, Yoshioka K, Kawano T, Tanaka Y, et al. The roles of intrahepatic Valpha14(+) NK1.1(+) T cells for liver injury induced by Salmonella infection in mice. Hepatology. 1999;29:1799–808.
27. Kaneko Y, Harada M, Kawano T, Yamashita M, Shibata Y, Gejyo F, et al. Augmentation of Valpha14 NKT cell-mediated cytotoxicity by interleukin 4 in an autocrine mechanism resulting in the development of concanavalin A-induced hepatitis. J Exp Med. 2000;191:105–14.
28. Osman Y, Kawamura T, Naito T, Takeda K, Van Kaer L, Okumura K, et al. Activation of hepatic NKT cells and subsequent liver injury following administration of alpha-galactosylceramide. Eur J Immunol. 2000;30:1919–28.
29. Wintermeyer P, Cheng CW, Gehring S, Hoffman BL, Holub M, Brossay L, et al. Invariant natural killer T cells suppress the neutrophil inflammatory response in a mouse model of cholestatic liver damage. Gastroenterology. 2009;136:1048–59.
30. Mantovani A, Sica A, Sozzani S, Allavena P, Vecchi A, Locati M. The chemokine system in diverse forms of macrophage activation and polarization. Trends Immunol. 2004;25:677–86.
31. Moser B, Wolf M, Walz A, Loetscher P. Chemokines: multiple levels of leukocyte migration control. Trends Immunol. 2004;25:75–84.
32. Bigorgne AE, Bouchet-Delbos L, Naveau S, Dagher I, Prévot S, Durand-Gasselin I, et al. Obesity-induced lymphocyte hyperresponsiveness to chemokines: a new mechanism of fatty liver inflammation in obese mice. Gastroenterology. 2008;134:1459–69.
33. Crispe IN. Hepatic T cells and liver tolerance. Nat Rev Immunol. 2003;3:51–62.
34. Gao B, Jeong WI, Tian Z. Liver: an organ with predominant innate immunity. Hepatology. 2008;47:729–36.
35. Paik YH, Schwabe RF, Bataller R, Russo MP, Jobin C, Brenner DA. Toll-like receptor 4 mediates inflammatory signaling by bacterial lipopolysaccharide in human hepatic stellate cells. Hepatology. 2003;37:1043–55.
36. Seki E, De Minicis S, Osterreicher CH, Kluwe J, Osawa Y, Brenner DA, et al. TLR4 enhances TGF-beta signaling and hepatic fibrosis. Nat Med. 2007;13:1324–32.
37. Lee JY, Hwang DH. The modulation of inflammatory gene expression by lipids: mediation through Toll-like receptors. Mol Cells. 2006;21:174–85.
38. Lee JY, Zhao L, Hwang DH. Modulation of pattern recognition receptor-mediated inflammation and risk of chronic diseases by dietary fatty acids. Nutr Rev. 2010;68:38–61.

The Bcl-xL Inhibitor, ABT-737, Efficiently Induces Apoptosis and Suppresses Growth of Hepatoma Cells in Combination with Sorafenib

Hayato Hikita,[1]* Tetsuo Takehara,[1]* Satoshi Shimizu,[1] Takahiro Kodama,[1] Minoru Shigekawa,[1] Kyoko Iwase,[1] Atsushi Hosui,[1] Takuya Miyagi,[1] Tomohide Tatsumi,[1] Hisashi Ishida,[1] Wei Li,[1] Tatsuya Kanto,[1] Naoki Hiramatsu,[1] and Norio Hayashi[2]

Tumor cells are characterized by uncontrolled proliferation, often driven by activation of oncogenes, and apoptosis resistance. The oncogenic kinase inhibitor sorafenib can significantly prolong median survival of patients with advanced hepatocellular carcinoma (HCC), although the response is disease-stabilizing and cytostatic rather than one of tumor regression. Bcl-xL (B cell lymphoma extra large), an antiapoptotic member of the B cell lymphoma-2 (Bcl-2) family, is frequently overexpressed in HCC. Here, we present *in vivo* evidence that Bcl-xL overexpression is directly linked to the rapid growth of solid tumors. We also examined whether ABT-737, a small molecule that specifically inhibits Bcl-xL but not myeloid cell leukemia-1 (Mcl-1), could control HCC progression, especially when used with sorafenib. Administration of ABT-737, even at an *in vivo* effective dose, failed to suppress Huh7 xenograft tumors in mice. ABT-737 caused the levels of Mcl-1 expression to rapidly increase by protein stabilization. This appeared to be related to resistance to ABT-737, because decreasing Mcl-1 expression levels to the baseline by a small interfering RNA–mediated strategy made hepatoma cells sensitive to this agent. Importantly, administration of ABT-737 to Mcl-1 knockout mice induced severe liver apoptosis, suggesting that tumor-specific inhibition of Mcl-1 is required for therapeutic purposes. Sorafenib transcriptionally down-regulated Mcl-1 expression specifically in tumor cells and abolished Mcl-1 up-regulation induced by ABT-737. Sorafenib, not alone but in combination with ABT-737, efficiently induced apoptosis in hepatoma cells. This combination also led to stronger suppression of xenograft tumors than sorafenib alone. *Conclusion:* Bcl-xL inactivation by ABT-737 in combination with sorafenib was found to be safe and effective for anti-HCC therapy in preclinical models. Direct activation of the apoptosis machinery seems to unlock the antitumor potential of oncogenic kinase inhibitors and may produce durable clinical responses against HCC. (HEPATOLOGY 2010;52:1310-1321)

The B cell lymphoma-2 (Bcl-2) family proteins regulate the mitochondrial pathway of apoptosis, a major form of cell death.[1] They include five antiapoptotic proteins, Bcl-2, B cell lymphoma extra large (Bcl-xL), myeloid cell leukemia-1 (Mcl-1), Bcl-2–related protien A1 (Bfl-1), and Bcl-2-like 2 (Bcl-w), and two structurally related proapoptotic proteins, Bcl-2–antagonist/killer (Bak) and Bcl-2–

Abbreviations: ALT, alanine aminotransferase; Bad, Bcl-2–associated agonist of cell death; Bak, Bcl-2–antagonist/killer; Bax, Bcl-2–associated X protein; Bcl-2, B cell lymphoma-2; BH3, Bcl-2 homology domain-3; Bid, BH3-interacting domain death agonist; cDNA, complementary DNA; HA, hemagglutinin; HCC, hepatocellular carcinoma; Mcl-1, myeloid cell leukemia-1; mRNA, messenger RNA; RT-PCR, reverse-transcription polymerase chain reaction; siRNA, small interfering RNA; USP9X, ubiquitin-specific peptidase 9 X-linked; WST, water-soluble tetrazolium.

From the [1]Department of Gastroenterology and Hepatology, Osaka University Graduate School of Medicine, Suita, Osaka, Japan; and [2]Kansai-Rosai Hospital, Amagasaki, Hyogo, Japan.

Received May 26, 2010; accepted June 30, 2010.

**These authors contributed equally to this work. This work was partly supported by a Grant-in-Aid for Scientific Research from the Ministry of Education, Culture, Sports, Science, and Technology, Japan (to Tetsuo Takehara) and Grant-in-Aid for Research on Hepatitis and BSE from the Ministry of Health, Labour and Welfare of Japan.*

Address reprint requests to: Tetsuo Takehara, M.D., Ph.D., Department of Gastroenterology and Hepatology, Osaka University Graduate School of Medicine, 2-2 Yamada-oka, Suita, Osaka 565-0871, Japan. E-mail: takehara@gh.med.osaka-u.ac.jp; fax: +81-6-6879-3629.

associated X protein (Bax), as well as several structurally diverse proapoptotic Bcl-2 homology domain-3 (BH3)-only proteins like Bcl-2–associated agonist of cell death (Bad), BH3-interacting domain death agonist (Bid), and Bcl-2-like 11 (Bim). Bak and Bax, effector molecules in this family, homo-oligomerize into proteolipid pores within the mitochondrial outer membrane, leading to release of cytochrome c followed by activation of downstream caspases, such as caspase-3/7, which dismantle a variety of cellular substrates, leading to cell death. Antiapoptotic Bcl-2 proteins function as regulators of apoptosis by directly or indirectly antagonizing Bak and Bax activity to maintain cellular integrity. BH3-only proteins, sensors of apoptosis, are activated by a variety of cellular stresses and either directly activate Bak and Bax or neutralize antiapoptotic Bcl-2 proteins, inducing cell death. Because tumor cells encounter a variety of cellular stresses, such as genotoxic and environmental factors, overexpression of antiapoptotic Bcl-2 family proteins is commonly observed and leads to survival of tumor cells.[2] We and others have reported that Bcl-xL is frequently overexpressed in human hepatocellular carcinomas (HCCs).[3–6] These reports point to the resistance of hepatoma cells to a wide variety of stress-inducing conditions. For example, Bcl-xL blocks p53-induced apoptosis in hepatoma cells, implying that Bcl-xL overexpression may be one of the mechanisms by which HCC survives under genotoxic conditions.[3] In addition, Bcl-xL overexpression was found to be associated with poor overall survival and disease-free survival after surgical resection for HCC.[7] These findings suggest that Bcl-xL may be a therapeutic target for HCC, although this possibility has not yet been addressed. Bcl-xL is also expressed in normal hepatocytes and plays a critical role in maintaining their integrity.[8] Thus, special caution is necessary when Bcl-xL inactivation is applied to therapeutic purposes.

Despite advances in understanding the mechanisms of cell death and the biology of Bcl-2 family proteins, therapeutic strategies for HCC targeting apoptotic molecules have been hampered due to a lack of specific inhibitors. ABT-737 is one of the first small-molecule inhibitors of Bcl-2 family proteins and opens the field for cancer treatment targeting the apoptosis machinery. ABT-737, designed as a Bad mimetic, binds and neutralizes Bcl-2, Bcl-xL, and Bcl-w, but not Mcl-1 or Bfl-1.[9-11] It has single-agent activity in a number of hematopoietic cancers and some solid tumors.[12,13] Its orally available derivative, ABT-263, is in early clinical trials against lymphoid malignancies, small-cell lung cancer, and chronic lymphocytic leukemia, with some promising results.[14] In this study, we investigated the impact of ABT-737 in treating human hepatoma in culture and using a xenograft model. We found that hepatoma cells are relatively resistant to ABT-737, presumably due to reciprocal up-regulation of Mcl-1 upon ABT-737 exposure. Although concomitant Mcl-1 inhibition appears to be effective for inducing apoptosis by ABT-737, it should be done in a tumor-specific manner, because administration of ABT-737 leads to liver deterioration in Mcl-1 knockout mice. Finally, sorafenib, an anti-HCC agent recently approved by the U.S. Food and Drug Administration, down-regulates Mcl-1 expression in a tumor-specific manner and induces apoptosis and tumor growth suppression in cooperation with ABT-737. Combination therapy with sorafenib and a Bcl-xL inhibitor seems to be an attractive strategy for controlling tumor progression in HCC.

Materials and Methods

Cell Lines and Reagents. Primary human hepatocytes were obtained from ScienCell Research Laboratories (Carlsbad, CA) and cultured with the provided medium. Human hepatoma cell lines were cultured with Dulbecco's modified Eagle medium (DMEM) supplemented with 10% heat-inactivated fetal bovine serum (Sigma, St. Louis, MO). Cycloheximide was purchased from Nacalai Tesque (Kyoto, Japan), sorafenib tablets were purchased from Bayer HealthCare (Osaka, Japan), and ABT-737 was kindly provided by Abbott Laboratories (Abbott Park, IL). They were dissolved with dimethyl sulfoxide for *in vitro* use.

Hela Cells Expressed Bcl-xL with the Tet-on System. pcDNA3HABcl-xL, an expression vector coding human Bcl-xL tagged with hemagglutinin (HA), was provided by Dr. G. Nunez (University of Michigan Medical School, Ann Arbor, MI). The pcDNA4/TOHABcl-xL was constructed by inserting the complementary DNA (cDNA) for Bcl-xL gene with HA-tag from pcDNA3HABcl-xL into the EcoRI site of pcDNA4/TO (Invitrogen, Carlsbad, CA). TREx-Hela cells (Invitrogen) were transfected with pcDNA4/

View this article online at wileyonlinelibrary.com.
DOI 10.1002/hep.23836
Potential conflict of interest: Nothing to report.
Additional Supporting Information may be found in the online version of this article.

TOHABcl-xL using Lipofectin (Invitrogen). The cells were cultured with DMEM containing 1.1 μg/mL zeocin, and zeocin-resistant clones were isolated. After examination of HA–Bcl-xL induction by doxycycline, two clones (Hela–Bcl-xL$^{Tet\text{-}on}$ clone A, clone B) were established and used for further experiments.

Mice. Conditional Bcl-xL knockout mice (*bcl-x$^{flox/flox}$ Alb-Cre* [albumin/cre recombinase]) and Mcl-1 knockout mice (*mcl-1$^{flox/flox}$ Alb-Cre*) were previously described.[15] Balb/c nude mice (CAnN.Cg-Foxn1^{nu}/CrlCrlj) were purchased from Charles River Laboratories (Yokohama, Japan). They were maintained in a specific pathogen–free facility and treated with humane care with approval from the Animal Care and Use Committee of Osaka University Medical School.

Apoptosis Assay. The *in vitro* apoptosis assay, measurement of caspase-3/7 activity, and the water-soluble tetrazolium salt (WST) assay, were described previously.[16] The *in vivo* apoptosis assay, measurement of serum alanine aminotransferase (ALT) level, and caspase-3/7 activity and histological analyses were also previously described.[15]

Western Blot Analysis. Whole-cell extracts from cultured cells or tissues were prepared and subjected to western blot. For immunodetection, the following antibodies were used: anti–Bcl-xL antibody and anti-human Mcl-1 antibody from Santa Cruz Biotechnology (Santa Cruz, CA); anti-mouse Mcl-1 antibody from Rockland (Gilbertsville, PA); anti-Bid antibody, anti-Bax antibody, and anti-cleaved caspase-3 antibody from Cell Signaling Technology (Beverly, MA); anti-Bak antibody from Millipore (Billerica, MA); anti-Bim antibody from Assay Design (Ann Arbor, MI); anti-ubiquitin-specific peptidase 9, X-linked (USP9X) antibody from Abnova (Taipei, Taiwan); and anti–beta actin antibody from Sigma-Aldrich (St. Louis, MO) or Cell Signaling Technology.

Xenograft Tumor. To produce a xenograft tumor, 3 × 10^6 to 5 × 10^6 Hela–Bcl-xL$^{Tet\text{-}on}$ clone A or Huh7 cells were subcutaneously injected to Balb/c nude mice. For induction of HA–Bcl-xL, the mice that were injected with Hela–Bcl-xL$^{Tet\text{-}on}$ clone A cells were fed with water containing 100 μg/mL doxycycline. For anticancer therapy, ABT-737 was administered as described.[17] Sorafenib tablets were crushed and orally administered with water containing 12.5% Cremophor EL (Sigma-Aldrich) and 12.5% ethanol. We estimated the volume of the xenograft tumor using the following formula: tumor volume = π/6 × (major axis) × (minor axis)^2.

Small RNA Interference. Hepatoma cell lines were transfected with Stealth select RNAi (set of three oligonucleotides, Invitrogen) RNA interference (RNAi) directed against Mcl-1 or USP9X. A Stealth RNAi negative control kit (set of three oligonucleotides, Invitrogen) was used as a control for sequence-independent effects following Stealth RNAi delivery. The transfections were carried out using Lipofectamine RNAiMAX (Invitrogen) according to the reverse transfection protocol.

Real-Time Reverse-Transcription Polymerase Chain Reaction. Real-time reverse-transcription PCR (RT-PCR) was performed as previously described.[15] Mcl-1 messenger RNA (mRNA) expressions were measured using TaqMan Gene Expression Assays (Assay ID: Hs03043899_m1) and were corrected with the quantified expression level of beta actin mRNA measured using TaqMan Gene Expression Assays (Assay ID: Hs99999903_m1).

Statistical Analysis. Data are presented as mean ± standard deviation. Differences between two groups were determined using the Student *t* test for unpaired observations unless otherwise noted. Multiple comparisons were performed by analysis of variance followed by Scheffe post hoc correction. $P < 0.05$ was considered statistically significant.

Results

Bcl-xL Overexpression Is a Molecular Mechanism of Rapid* In Vivo *Tumor Growth. Research has shown that Bcl-xL overexpression confers resistance to apoptosis in a variety of tumor cells. To examine its impact on tumor growth *in vivo*, we generated the Hela–Bcl-xL$^{Tet\text{-}on}$ cell line which expresses the modified tetracycline repressor molecule (rtTA) and Bcl-xL under control of tetracycline-responsive cis-elements. We chose Hela cells as a model because they expressed a relatively small amount of Bcl-xL in comparison with human hepatoma cells including Huh7, Hep3B, and HepG2 (Fig. 1A). Tetracycline analogue doxycycline treatment efficiently induced Bcl-xL in Hela–Bcl-xL$^{Tet\text{-}on}$ cells as expected (Fig. 1B) and conferred resistance to apoptosis as evidenced by significantly lower levels of caspase-3/7 activity in culture (Fig. 1C), although it did not have a significant effect on cell growth assay (Fig. 1D). Next, we subcutaneously injected Hela–Bcl-xL$^{Tet\text{-}on}$ cells into nude mice. When subcutaneous tumors grew to approximately 1 cm, the mice were randomly assigned to two groups: a doxycycline-drinking group and a water-drinking group. Subcutaneous tumors grew rapidly in the doxycycline-drinking group compared with the water-drinking group (Fig. 1E). As expected, xenograft tumors displayed higher levels of Bcl-xL expression than those in the water drinking group (Fig.

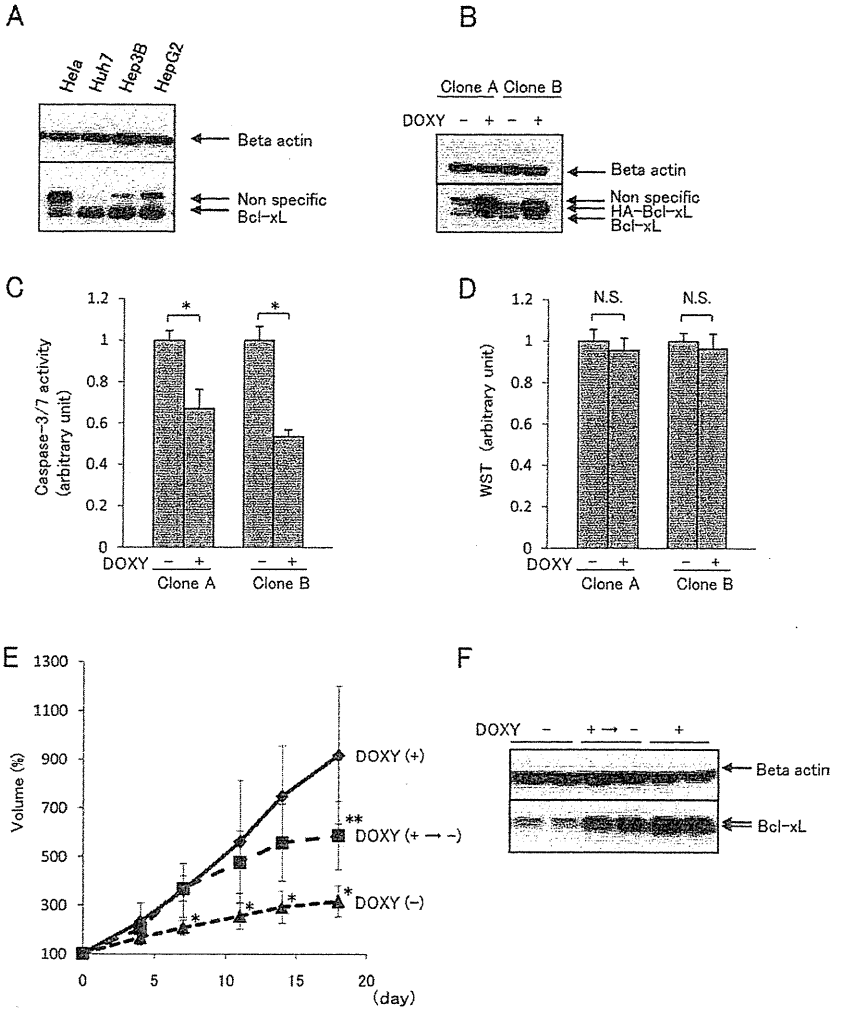

Fig. 1. Bcl-xL overexpression in vitro and in vivo by the Tet-on system. (A) Western blot analysis of Bcl-xL in human hepatoma cells and Hela cells. (B,C,D) Bcl-xL overexpression in vitro. Two independent clones of Hela-Bcl-xLTet-on cells were cultured with or without 1 μM doxycycline (DOXY) for 24 hours. (B) Western blot analysis of Bcl-xL. (C,D) Caspase-3/7 activity in culture supernatant and cell viability by the WST assay (N = 4). *P < 0.05. N.S., not significant. (E,F) Bcl-xL overexpression in vivo. Nude mice carrying xenograft tumors of Hela-Bcl-xL$^{Tet\text{-}on}$ clone A were randomly assigned to water given with or without 100 mg/mL doxycycline for 7 days. After 7 days, the mice of the doxycycline-drinking group were randomly assigned to two groups: one in which doxycycline drinking was continued and the other in which water was given instead (N = 5 or 6 per group). (E) The percentage of xenograft tumor volume. (F) Western blot analysis of xenograft tumor for the expression of Bcl-xL. *P < 0.05 versus the other two groups. **P < 0.05 versus the DOXY (+) group.

1F). In addition, switching the mice to water drinking at 7 days after doxycycline drinking decreased Bcl-xL expression and retarded tumor growth compared with continuing doxycycline drinking (DOXY + → − versus DOXY +, respectively; Fig. 1F). These results indicate that Bcl-xL overexpression was directly linked to rapid growth of tumors *in vivo* and suggest that Bcl-xL may be a therapeutic target for inhibiting tumor progression, especially for Bcl-xL–overexpressing tumors.

Bcl-xL Inhibitor ABT-737 Dose-Dependently Induces Apoptosis of Hepatoma Cells but Fails to Suppress Tumor Growth in a Xenograft Model. To examine the impact of pharmaceutical inactivation of Bcl-xL overexpressed in hepatoma cells, Huh7 and Hep3B hepatoma cells were cultured with escalating doses of ABT-737. ABT-737 dose-dependently activated caspase-3/7 in hepatoma cells and suppressed tumor growth at high dosages (Fig. 2A,B). To examine the *in vivo* effect of ABT-737, nude mice were subcutaneously injected with Huh7 cells to generate xenograft tumors and were randomly assigned into two groups when the diameter of the subcutaneous tumors reached approximately 1 cm: ABT-737 injection group and vehicle injection group. Administration of ABT-737 at 50 mg/kg body weight/day for 7 days failed to suppress tumor growth (Fig. 2C). In contrast, mild ALT elevation and thrombocytopenia were observed in ABT-737–injected mice (Fig. 2D). Previous research has demonstrated that both are observed in mice after ABT-737 administration,[17,18] confirming that the dose injected in the present experiment is sufficient for inducing a biological effect of ABT-737 *in vivo*.

ABT-737 Posttranscriptionally Increases Expression of Mcl-1. To examine the mechanisms underlying relative resistance of hepatoma cells to ABT-737, we examined the expression profile of the Bcl-2 family

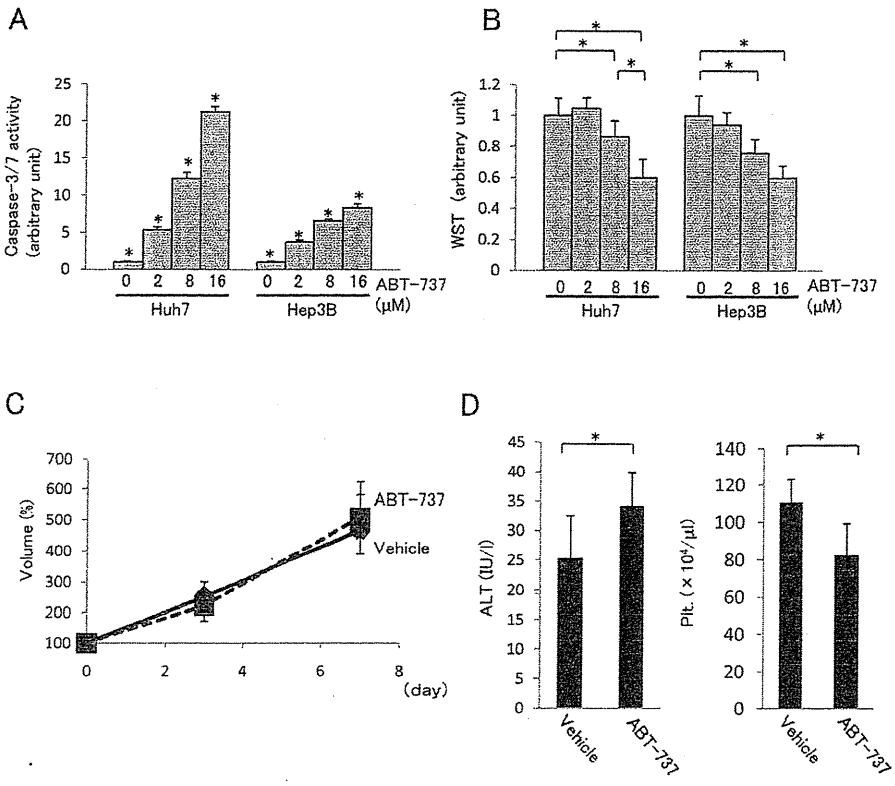

Fig. 2. Apoptosis and growth of hepatoma cells treated with ABT-737 *in vitro* and *in vivo*. (A,B) Huh7 and Hep3B cells were treated with indicated doses of ABT-737 for 24 hours (N = 4). (A) Caspase-3/7 activity of culture supernatant. $*P < 0.05$ versus all other groups. (B) Cell viability by the WST assay. $*P < 0.05$. (C,D) Nude mice carrying xenograft tumors of Huh7 cells were intraperitoneally administered 50 mg/kg ABT-737 or vehicle daily for 7 days. (N = 9 for each group.) (C) The percentage of xenograft tumor volume. (D) Serum ALT levels and circulating platelet count. $*P < 0.05$.

proteins. Administration of ABT-737 did not affect expression of proapoptotic multidomain members Bak and Bax or BH3-only proteins Bid and Bim in cultured hepatoma cell lines Huh7 and Hep3B (Fig. 3A). Although the slower migrating species of Bim at 4 hours was increased, this change disappeared at 24 hours. In agreement with previous research,[19,20] Mcl-1 was constitutively expressed in hepatoma cells. Of importance is the finding that the levels of Mcl-1 expression were rapidly increased as early as 4 hours after ABT-737 exposure. Expression of mcl-1 mRNA did not differ between ABT-737–treated cells and vehicle-treated cells (Fig. 3B), suggesting the involvement of a posttranscriptional mechanism. Because Mcl-1 is a rapid-turnover protein, the levels of Mcl-1 may be regulated by protein degradation.[21] To examine this, we treated hepatoma cells with cycloheximide, a well-established protein synthesis inhibitor, in the presence or absence of ABT-737. Cycloheximide-induced rapid decline in Mcl-1 expression was substantially blocked in the presence of ABT-737, suggesting that ABT-737 significantly delays degradation and prolongs the stability of Mcl-1 (Fig. 3C). Recently, it was reported that the deubiquitinase USP9X is involved in stabilization of Mcl-1.[22] In this study, western blot analysis revealed that the levels of USP9X expression were not changed in Huh7 and Hep3B with ABT-737 (Supporting Fig. 1A). Furthermore, USP9X down-regulation by small interfering RNA (siRNA) could not block the Mcl-1 up-regulation induced by ABT-737 (Supporting Fig. 1B).These results suggest that USP9X was not involved in Mcl-1 up-regulation induced by ABT-737. Of importance is the finding that Mcl-1 expression was also up-regulated after administration of ABT-737 in our xenograft model (Fig. 3D). Because Mcl-1 is not a target of ABT-737, relative resistance to ABT-737 of hepatoma cells may be due, at least in part, to posttranscriptional induction of Mcl-1.

Mcl-1 Knockdown Sensitizes Hepatoma Cells to ABT-737. To examine the impact of Mcl-1 induction in hepatoma cell resistance to ABT-737, we silenced Mcl-1 expression through use of three different siRNAs. Western blot analysis revealed that Mcl-1 siRNA2 and siRNA3 completely knocked down Mcl-1 expression in Hep3B cells, whereas Mcl-1 siRNA1 did so only partially (Fig. 4A). Mcl-1 knockdown or a medium dose of ABT-737 (4 μM) modestly activated caspase-3/7 in Hep3B cells, whereas both substantially activated caspase-3/7 (Fig. 4B). In addition, Mcl-1 knockdown or ABT-737 alone failed to suppress the growth of tumor cells but caused significant suppression when used together (Fig. 4C). Caspase-3 activation was also confirmed by western blots (Fig. 4A). It should be noted that Mcl-1 siRNA1 reduced Mcl-1

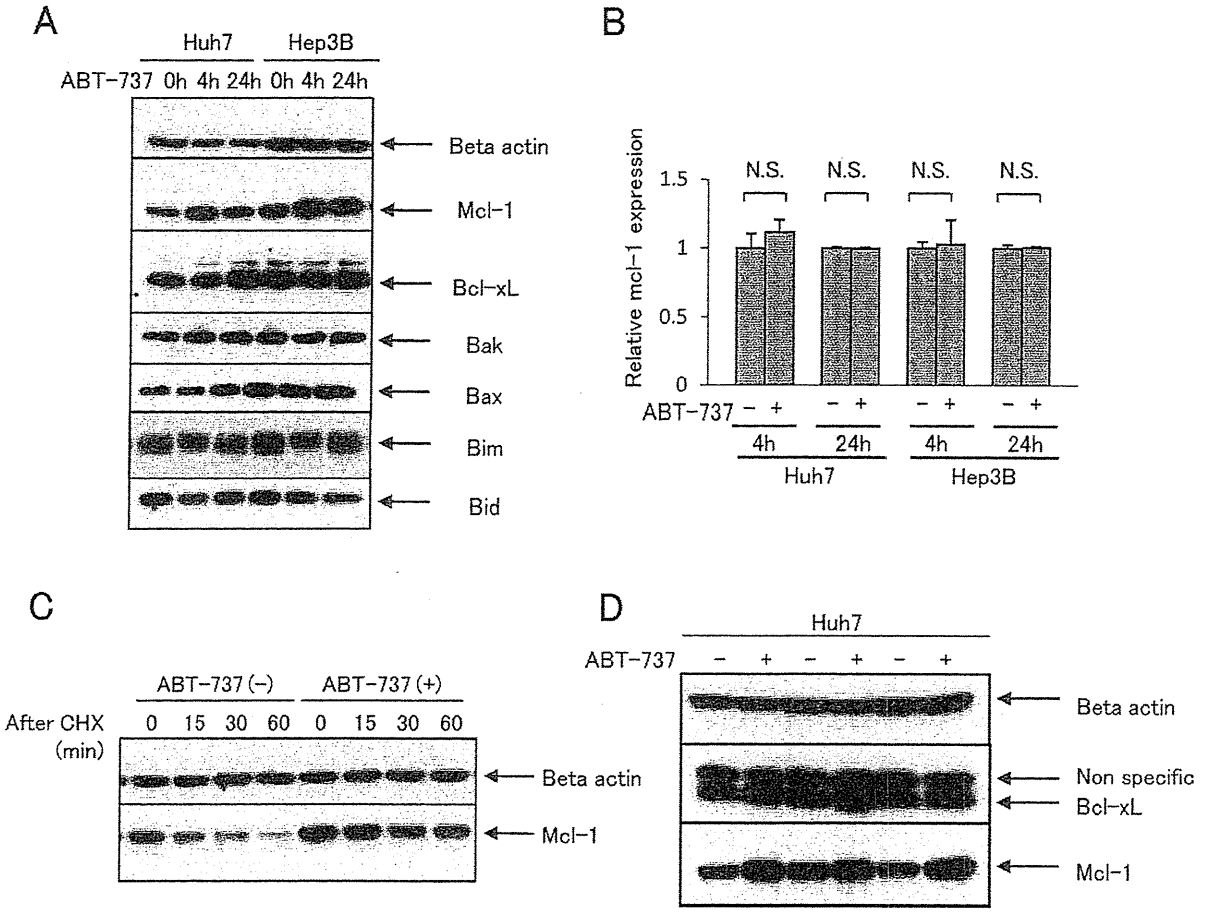

Fig. 3. Up-regulation of Mcl-1 in human hepatoma cells by ABT-737 in vitro and in vivo. (A,B) Huh7 and Hep3B cells were cultured with 4 μM ABT-737 for the indicated times. (A) Western blot analysis for the expression of Bcl-2 family proteins. (B) Real-time RT-PCR analysis for mcl-1 mRNA expression (N = 6). The levels were normalized to each group without ABT-737. N.S., not significant. (C) Huh7 cells were cultured with or without 4 μM ABT-737 for 4 hours and then further treated with 1 mM cycloheximide (CHX) for the indicated times. Western blot analysis for Mcl-1 expression. (D) Nude mice carrying xenograft tumors of Huh7 cells were intraperitoneally administered 50 mg/kg ABT-737 or vehicle daily for 7 days. Western blot analysis of xenograft tumor after 7-day treatment for the expression of Bcl-2 family proteins.

expression in ABT-737-treated cells to levels similar to those of untreated cells (Fig. 4A). Even in this case, mcl-1 knockdown enhanced caspase activation and growth suppression of Hep3B cells induced by ABT-737. Similar data were obtained with another hepatoma cell line, Huh7 (Fig. 4A and Supporting Fig. 2). These results indicate that Mcl-1 up-regulation induced by ABT-737 is involved in the resistance of hepatoma cells to ABT-737 and suggest that combination therapy with ABT-737 and Mcl-1 inhibitor may be predictably effective *in vivo*.

We previously reported that, similar to Bcl-xL, Mcl-1 plays an important role in apoptosis resistance of normal hepatocytes. In addition, knockdown of both Mcl-1 and Bcl-xL led to impaired liver development during embryogenesis.[15] Thus, the concern arises that simultaneous inactivation of both Bcl-xL and Mcl-1 may cause severe liver injury in adults. To examine this possibility, we injected ABT-737 into hepatocyte-specific Mcl-1 knockout mice or wild-type littermates. ABT-737 injection into wild-type mice led to mild liver apoptosis, which is consistent with our previous finding,[17] whereas injection into Mcl-1 knockout mice induced massive liver apoptosis leading to severe liver injury, and most animals died within 1 day (Fig. 4D,E). This result indicates that inactivation of both Bcl-xL and Mcl-1 may be hazardous and that Mcl-1 inactivation should be done in a tumor-specific manner.

Sorafenib Down-Regulates Mcl-1 Expression in Hepatoma Cells Much More Strongly than in Normal Liver Cells. Previous research has shown that sorafenib down-regulates Mcl-1 expression in hepatoma cells in a mitogen-activated protein kinase/extracellular signal-regulated kinase (MEK/ERK)-independent manner.[16,23] In the present study, to examine whether Mcl-1

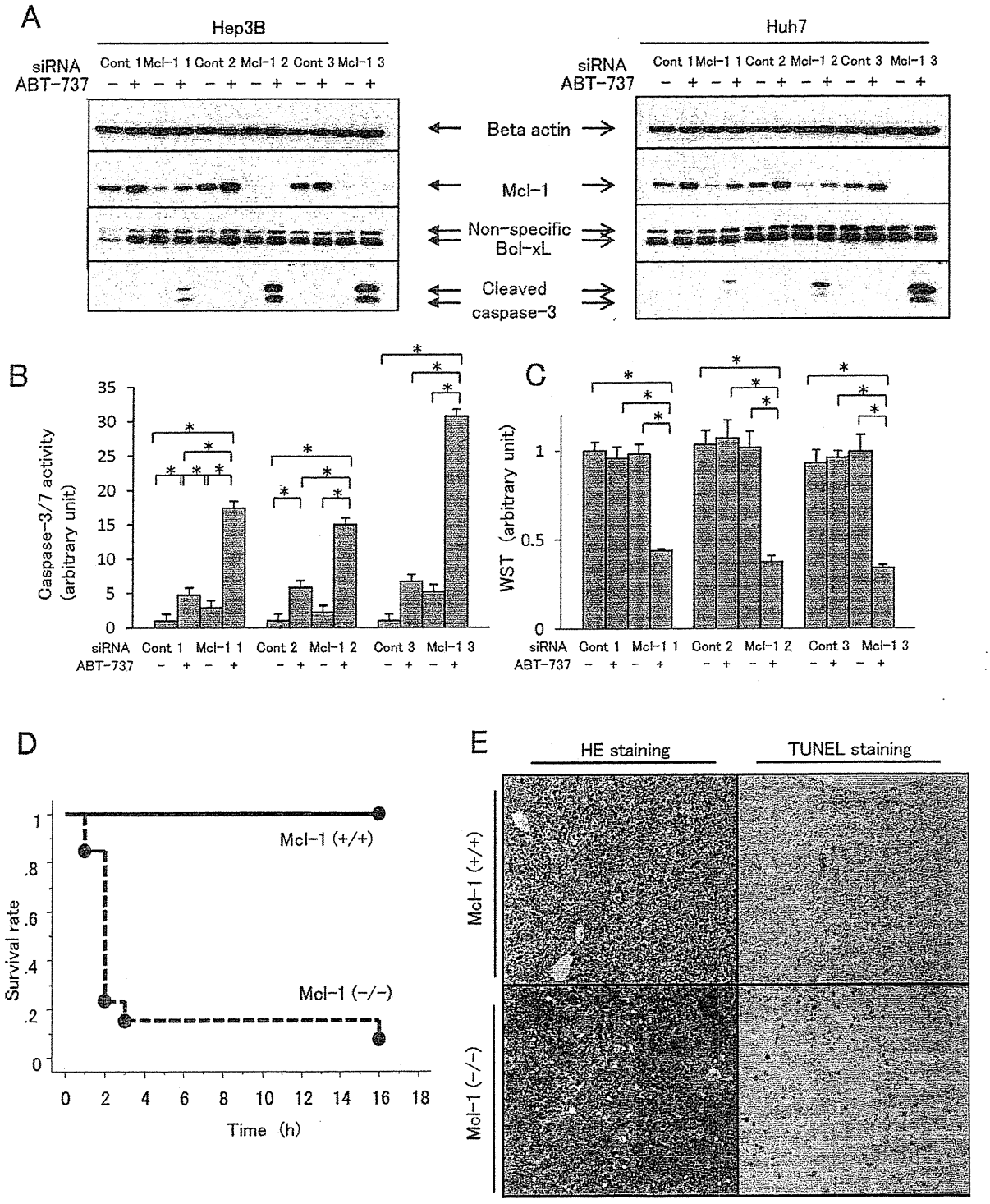

Fig. 4. Effects of ABT-737 under inhibition of Mcl-1 in vitro and in vivo. (A-C) Hep3B and Huh7 cells were transfected with Mcl-1 siRNAs (Mcl-1 1, Mcl-1 2, and Mcl-1 3) or control siRNAs (Cont 1, Cont 2, Cont 3). Forty-eight hours after transfection, they were treated with or without 4 μM ABT-737 for 24 hours (N = 4). (A) Western blot analysis for the expression of Mcl-1, Bcl-xL, and cleaved caspase-3. (B) Caspase-3/7 activities of supernatant in Hep3B culture dishes. *P < 0.05. (C) Cell viability of Hep3B cells by the WST assay. *P < 0.05. (D,E) Wild-type mice (Mcl-1 +/+) and hepatocyte-specific Mcl-1 knockout mice (Mcl-1 −/−) were intraperitoneally administered 50 mg/kg of ABT-737. (D) Survival curve of the mice (N = 13 or 15). (E) Hematoxylin and eosin (HE) and terminal deoxynucleotidyl transferase-mediated deoxyuridine triphosphate nick-end labeling (TUNEL) staining of the liver sections 16 hours after administration of ABT-737 with wild-type mice and immediately after death with Mcl-1 knockout mice. Representative photographs are shown.

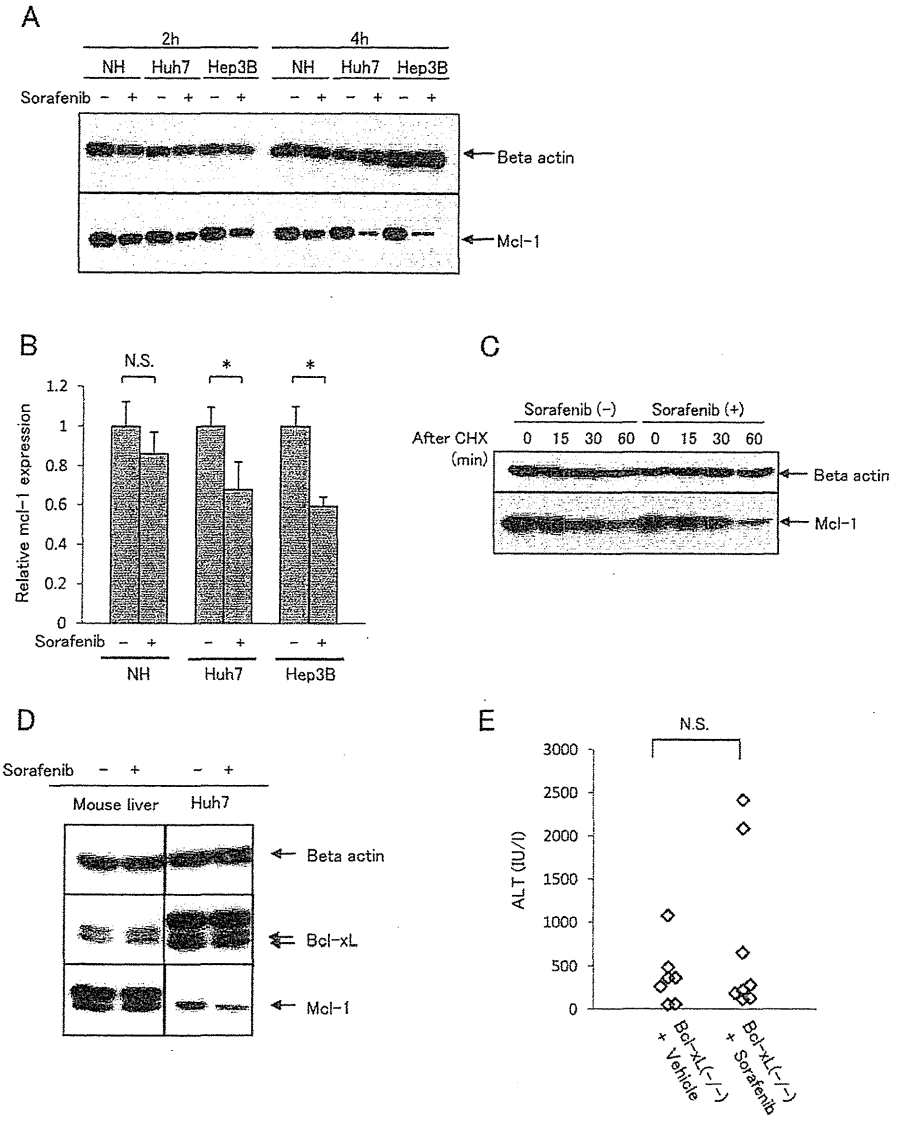

Fig. 5. Effects of sorafenib on the Mcl-1 expression in hepatoma cells and nontransformed cells in vitro and in vivo. (A,B) Normal hepatocytes (NH) and Huh7 and Hep3B cells were treated with 5 μM sorafenib. (A) Western blot analysis for the expression of Mcl-1 after treatment for 2 or 4 hours. (B) Real-time RT-PCR analysis for mcl-1 expression after treatment for 4 hours (N = 6). The levels were normalized to each group without sorafenib. N.S., not significant. *P < 0.05. (C) Huh7 cells were cultured with 1 mM cycloheximide (CHX) with or without 5 μM sorafenib for the indicated times. Western blot analysis for Mcl-1 expression. (D) Nude mice carrying xenograft tumors of Huh7 cells were orally administered 30 mg/kg sorafenib or vehicle daily for 3 days. Western blot analysis for the expression of Bcl-xL and Mcl-1 in the xenograft tumor of Huh7 cells and the liver of mice. (E) Hepatocyte-specific Bcl-xL knockout mice (Bcl-xL −/−) were orally administered daily 30 mg/kg sorafenib or vehicle daily for 3 days. The serum ALT levels are shown (N = 7 or 8). The difference between two groups was determined using Mann-Whitney's U test. N.S., not significant.

suppression of sorafenib is tumor-specific, nontransformed human hepatocytes and hepatoma cell lines were treated with sorafenib. Sorafenib down-regulated Mcl-1 expression in all hepatoma cell lines tested, but had a lesser effect on nontransformed human hepatocytes (Fig. 5A). Sorafenib down-regulated mcl-1 mRNA expression in Huh7 and Hep3B hepatoma cells but not in nontransformed hepatocytes (Fig. 5B). To examine the posttranscriptional effect of sorafenib for Mcl-1 expression, we treated Huh7 cells with cycloheximide in the presence or absence of sorafenib. Cycloheximide-induced decline in Mcl-1 expression was not accelerated by sorafenib (Fig. 5C). This result indicated that, in contrast to the case of ABT-737, sorafenib does not affect the degradation process of Mcl-1.

We also examined Mcl-1 expression in the liver as well as xenograft tumors. Administration of sorafenib significantly suppressed Mcl-1 expression in Huh7 xenograft tumors but not in the liver (Fig. 5D). To examine the safety of sorafenib in the absence of Bcl-xL *in vivo*, we administered sorafenib to hepatocyte-specific Bcl-xL knockout mice. These mice had elevated levels of serum ALT at baseline, as we reported previously,[8] but displayed neither further ALT elevation nor lethal liver failure upon sorafenib administration (Fig. 5E). Taken together, these results indicate that sorafenib did not affect Mcl-1 expression in the liver and therefore did not cause further liver injury even if Bcl-xL was inactivated.

ABT-737 Induced Apoptosis of Hepatoma Cells and Suppressed Growth of Xenograft Tumor with Sorafenib Coadministration. To examine the impact of coadministration of sorafenib and ABT-737 on

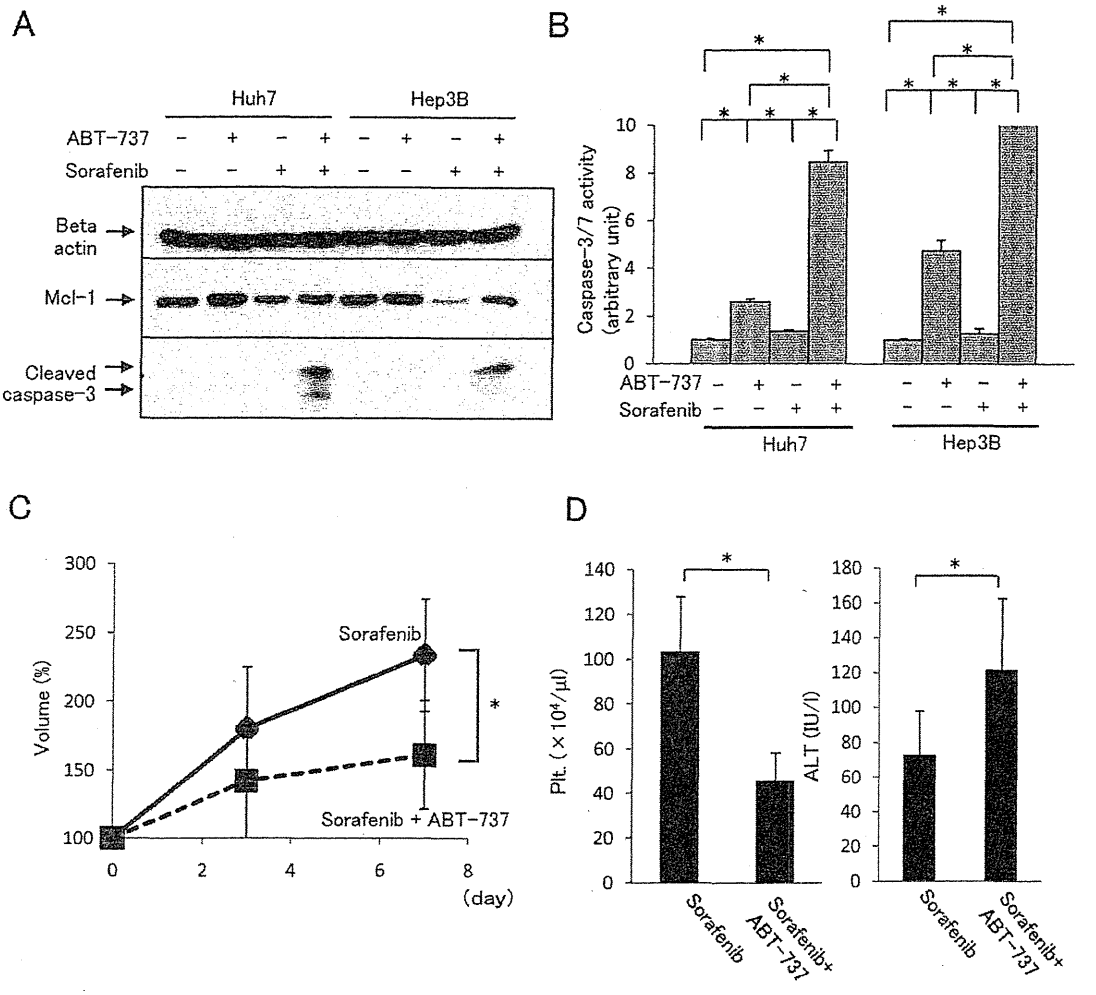

Fig. 6. Effects of ABT-737 with sorafenib treatment in vitro and in vivo. (A,B) Huh7 and Hep3B cells were treated with or without 4 μM ABT-737 together with or without 5 μM sorafenib. (A) Western blot analysis for the expression of Mcl-1 and cleaved caspase-3. (B) Caspase-3/7 activity of culture supernatants. *$P < 0.05$. (C,D) Nude mice carrying xenograft tumors of Huh7 cells were intraperitoneally administered daily 50 mg/kg ABT-737 or vehicle with daily oral administration of 30 mg/kg sorafenib for 7 days ($N = 8$ or 11). (C) The percentage of xenograft tumor volume. (D) Circulating platelet (Plt.) count and serum ALT levels. *$P < 0.05$.

inducing apoptosis, we treated Huh7 and Hep3B hepatoma cells with ABT-737 and/or sorafenib. Although ABT-737 up-regulated Mcl-1 expression in Huh7 and Hep3B cells, sorafenib abolished the Mcl-1 up-regulation induced by ABT-737; the levels of Mcl-1 expression of cells treated with both were similar to those of nontreated cells (Fig. 6A). Sorafenib failed to activate caspase-3/7 in hepatoma cells by itself, but efficiently activated it in the presence of ABT-737 (Fig. 6B). It was also confirmed by efficient cleavage of caspase-3 on western blot analysis (Fig. 6A).

To examine whether ABT-737 has an antitumor effect in the presence of sorafenib, we administered ABT-737 and sorafenib together to nude mice bearing Huh7 xenograft tumors. Although even sorafenib alone significantly suppressed tumor growth compared with the vehicle alone (Supporting Fig. 3), coadministration of ABT-737 and sorafenib led to significant further suppression of tumor growth compared to administration of sorafenib alone (Fig. 6C). Similar to administration of ABT-737 as a single agent, coadministration of sorafenib and ABT-737 also induced mild thrombocytopenia and ALT elevation (Fig. 6D). However, coadministration did not induce further morbidity or mortality in mice, suggesting that this regimen is safe and effective for controlling HCC progression.

Discussion

Tumor cells have two characteristic features: uncontrolled proliferation and apoptosis resistance. Uncontrolled proliferation, driven by activation of a variety

of oncogenes, is directly linked to tumor growth. Apoptosis resistance is believed to be required for the oncogene-induced aberrant proliferation, because without it, tumor cells tend to undergo apoptosis.[24] However, the direct link between apoptosis resistance and growth of solid tumors *in vivo* has not been well studied. Clarifying this point is very important, especially because a very recent study by Weber et al.[25] produced the contradictory finding that aged hepatocyte-specific Mcl-1 knockout mice develop HCC-like lesions, suggesting a link between hepatocarcinogenesis and increased proliferation resulting from increased apoptosis. In the present study, we used conditional expression of Bcl-xL in tumor cells to show that Bcl-xL overexpression, which is frequently found in human HCC, can be directly linked to tumor growth *in vivo*, although it did not promote significant cell growth *in vitro*. Our results suggest that tumor cells encounter a variety of cellular stresses and require antiapoptosis to survive *in vivo* rather than *in vitro*. Thus, we consider antiapoptosis to be an important mechanism for progression of a solid tumor, even if it may not be the case for tumor development as suggested by Weber et al.[25] Our finding also provides proof of the concept that Bcl-xL may be a target for therapy against HCC progression.

In the present study, we showed that, unlike hematopoietic malignancy, hepatoma cells are relatively resistant to ABT-737. Although ABT-737 dose-dependently induced apoptosis in hepatoma cells, a relatively high dose of ABT-737 (more than 8 μM) was required to suppress tumor growth *in vitro*. Importantly, administration of an *in vivo* effective dose of ABT-737 (50 mg/kg) failed to suppress xenograft tumors. We found increased expression of Mcl-1 in cultured hepatoma cells as well as xenograft tumors upon ABT-737 treatment. This may be part of the mechanism of their relative resistance to ABT-737 because hepatoma cells were highly sensitive to this agent if Mcl-1 expression levels were kept constant by an siRNA strategy. Previous articles have reported that Mcl-1 knockdown makes some tumor cells sensitive to ABT-737.[26,27] The present study showed that ABT-737 up-regulation of Mcl-1 rather than Mcl-1 expression itself may be a mechanism of tumor cell resistance to this agent.

A recent study demonstrated that long-term exposure to ABT-737 made initially sensitive lymphoma cell lines resistant to this agent via up-regulation of Mcl-1.[28] In this study, Mcl-1 up-regulation in the ABT-737–resistant lymphoma cells were reported to be mediated by transcriptional up-regulation. In the present study, hepatoma cells showed immediate, posttranscriptional up-regulation of Mcl-1. This rapid response may contribute to the difficulty of treating hepatoma cells with ABT-737 compared with lymphoma cells in which ABT-737 is reported to be effective not only *in vitro*[29] but also *in vivo*.[30] The mechanism by which hepatoma cells posttranscriptionally up-regulate Mcl-1 upon ABT-737 exposure is not clear at present. However, our study has shown that Mcl-1 up-regulation was mediated by delayed degradation of Mcl-1 protein in ABT-737–treated cells without involving the USP9X deubiquitinase. ABT-737 is a Bad mimetic small molecule and preferentially binds with the BH3-binding groove of Bcl-xL. This binding may release endogenous BH3-only proteins such as Bim and Bid and presumably Bak and Bax from Bcl-xL and these unleashed Bcl-2 proteins may then bind Mcl-1. The interaction between Mcl-1 and the unleashed Bcl-2 proteins may cause increased Mcl-1 stability. Because Bak/Bax and Bid/Bim function as effectors and activators for the mitochondrial pathway of apoptosis, respectively, their binding with Mcl-1 may also cause apoptosis resistance to ABT-737.

Not only efficacy but also safety is an important point when considering a therapeutic strategy for cancer. Tumor cells sometimes share similar mechanisms for survival with normal cells. Indeed, HCCs overexpress Bcl-xL, but this molecule also plays an important role in maintaining the integrity of normal hepatocytes.[8] In the present study, we administered ABT-737 to Mcl-1 knockout mice and demonstrated that inactivation of both Bcl-xL and Mcl-1 could induce lethal hepatitis. We previously reported that Bcl-xL and Mcl-1 are required for liver development during embryogenesis,[15] and the present study also revealed the critical importance of both molecules in the adult liver. Recently, the possibility of combination therapy for down-regulation of Bcl-xL and Mcl-1 has been reported *in vitro*.[26,27,31] The present study, for the first time, focused on the *in vivo* safety of this strategy.

Regarding safety concerns about the inactivation of both Mcl-1 and Bcl-xL, sorafenib is an attractive agent because as we have revealed in this study, it down-regulates Mcl-1 expression in a relatively specific manner in tumor cells. Experiments with sorafenib administration into Bcl-xL knockout mice confirmed the safety of coadministration of sorafenib and ABT-737. The underlying mechanisms by which sorafenib down-regulates Mcl-1 in a tumor-specific manner are not clear. Some reports have shown that the down-regulation of Mcl-1 by sorafenib is independent of MEK/ERK,[16,23,32] but is dependent on Raf, AKT (protein kinase B), and Tyr705 phosphorylation of signal transducer and activator of transcription 3 (STAT3).[33,34]

Together with the report that activation of Ras/Raf and STAT3 pathways was found in HCC,[35] these pathways in tumor cells may be more activated than in healthy cells and result in the specificity of Mcl-1 down-regulation in tumor cells by sorafenib. Further experiments are needed to clarify this point.

Sorafenib belongs to a recently approved new class of targeted therapeutics that inhibit the oncogenic kinase pathway for HCC. It has been found to significantly prolong survival of patients with advanced HCC, although its effect appeared to be one of maintaining a stable disease state rather than inducing tumor regression.[36,37] It is speculated that sorafenib produces anticancer effects through a variety of ways such as suppression of angiogenesis and cell cycle arrest of tumor cells. Although it down-regulates Mcl-1,[16,23,32-34] its effect on apoptosis has not been clearly understood. In the present study, we found that sorafenib could not efficiently induce apoptosis in hepatoma cells by itself. This might explain why this agent elicits predominantly disease-stabilizing, cytostatic responses rather than tumor regression. Adding ABT-737 efficiently induced apoptosis of hepatoma cells, clearly indicating that the target of ABT-737, presumably Bcl-xL, blocks the apoptosis-inducing potency of sorafenib. Furthermore, coadministration of ABT-737 and sorafenib led to stronger suppression of xenograft tumor growth than did administration of sorafenib alone. These results suggest that combining sorafenib with ABT-737 may be an attractive strategy for producing durable clinical responses to combat HCC.

In conclusion, we have demonstrated that the inhibition of Bcl-xL by ABT-737 under sorafenib administration was safe and effective for anti-HCC therapy in preclinical models. ABT-737, a direct activator of apoptosis machinery, may unlock the potent antitumor potential of oncogenic kinase inhibitors such as sorafenib.

Acknowledgment: We sincerely thank Abbott Laboratories for providing ABT-737, Dr. You-Wen He (Department of Immunology, Duke University Medical Center, Durham, NC) for providing the *mcl-1* floxed mice and Dr. Lothar Hennighausen (Laboratory of Genetics and Physiology, National Institute of Diabetes and Digestive and Kidney Diseases, National Institutes of Health, Bethesda, MD) for providing the *bcl-x* floxed mice.

References

1. Tsujimoto Y. Cell death regulation by the Bcl-2 protein family in the mitochondria. J Cell Physiol 2003;195:158-167.
2. Yip KW, Reed JC. Bcl-2 family proteins and cancer. Oncogene 2008; 27:6398-6406.
3. Takehara T, Liu X, Fujimoto J, Friedman SL, Takahashi H. Expression and role of Bcl-xL in human hepatocellular carcinomas. HEPATOLOGY 2001;34:55-61.
4. Watanabe J, Kushihata F, Honda K, Mominoki K, Matsuda S, Kobayashi N. Bcl-xL overexpression in human hepatocellular carcinoma. Int J Oncol 2002;21:515-519.
5. Takehara T, Takahashi H. Suppression of Bcl-xL deamidation in human hepatocellular carcinomas. Cancer Res 2003;63:3054-3057.
6. Ding ZB, Shi YH, Zhou J, Qiu SJ, Xu Y, Dai Z, et al. Association of autophagy defect with a malignant phenotype and poor prognosis of hepatocellular carcinoma. Cancer Res 2008;68:9167-9175.
7. Watanabe J, Kushihata F, Honda K, Sugita A, Tateishi N, Mominoki K, et al. Prognostic significance of Bcl-xL in human hepatocellular carcinoma. Surgery 2004;135:604-612.
8. Takehara T, Tatsumi T, Suzuki T, Rucker EB 3rd, Hennighausen L, Jinushi M, et al. Hepatocyte-specific disruption of Bcl-xL leads to continuous hepatocyte apoptosis and liver fibrotic responses. Gastroenterology 2004;127:1189-1197.
9. Oltersdorf T, Elmore SW, Shoemaker AR, Armstrong RC, Augeri DJ, Belli BA, et al. An inhibitor of Bcl-2 family proteins induces regression of solid tumours. Nature 2005;435:677-681.
10. Vogler M, Dinsdale D, Dyer MJ, Cohen GM. Bcl-2 inhibitors: small molecules with a big impact on cancer therapy. Cell Death Differ 2009;16:360-367.
11. Mott JL, Gores GJ. Piercing the armor of hepatobiliary cancer: Bcl-2 homology domain 3 (BH3) mimetics and cell death. HEPATOLOGY 2007;46:906-911.
12. Del Gaizo Moore V, Schlis KD, Sallan SE, Armstrong SA, Letai A. BCL-2 dependence and ABT-737 sensitivity in acute lymphoblastic leukemia. Blood 2008;111:2300-2309.
13. Hann CL, Daniel VC, Sugar EA, Dobromilskaya I, Murphy SC, Cope L, et al. Therapeutic efficacy of ABT-737, a selective inhibitor of BCL-2, in small cell lung cancer. Cancer Res 2008;68:2321-2328.
14. Tse C, Shoemaker AR, Adickes J, Anderson MG, Chen J, Jin S, et al. ABT-263: a potent and orally bioavailable Bcl-2 family inhibitor. Cancer Res 2008;68:3421-3428.
15. Hikita H, Takehara T, Shimizu S, Kodama T, Li W, Miyagi T, et al. Mcl-1 and Bcl-xL cooperatively maintain integrity of hepatocytes in developing and adult murine liver. HEPATOLOGY 2009;50:1217-1226.
16. Shimizu S, Takehara T, Hikita H, Kodama T, Miyagi T, Hosui A, et al. The let-7 family of microRNAs negatively regulates Bcl-xL expression and potentiates sorafenib-induced apoptosis in human hepatocellular carcinoma. J Hepatol 2010;52:698-704.
17. Hikita H, Takehara T, Kodama T, Shimizu S, Hosui A, Miyagi T, et al. BH3-only protein bid participates in the Bcl-2 network in healthy liver cells. HEPATOLOGY 2009;50:1972-1980.
18. Mason KD, Carpinelli MR, Fletcher JI, Collinge JE, Hilton AA, Ellis S, et al. Programmed anuclear cell death delimits platelet life span. Cell 2007;128:1173-1186.
19. Sieghart W, Losert D, Strommer S, Cejka D, Schmid K, Rasoul-Rockenschaub S, et al. Mcl-1 overexpression in hepatocellular carcinoma: a potential target for antisense therapy. J Hepatol 2006;44:151-157.
20. Fleischer B, Schulze-Bergkamen H, Schuchmann M, Weber A, Biesterfeld S, Müller M, et al. Mcl-1 is an anti-apoptotic factor for human hepatocellular carcinoma. Int J Oncol 2006;28:25-32.
21. Zhong Q, Gao W, Du F, Wang X. Mule/ARF-BP1, a BH3-only E3 ubiquitin ligase, catalyzes the polyubiquitination of Mcl-1 and regulates apoptosis. Cell 2005;121:1085-1095.
22. Schwickart M, Huang X, Lill JR, Liu J, Ferrando R, French DM, et al. Deubiquitinase USP9X stabilizes MCL1 and promotes tumour cell survival. Nature 2010;463:103-107.
23. Liu L, Cao Y, Chen C, Zhang X, McNabola A, Wilkie D, et al. Sorafenib blocks the RAF/MEK/ERK pathway, inhibits tumor angiogenesis, and induces tumor cell apoptosis in hepatocellular carcinoma model PLC/PRF/5. Cancer Res 2006;66:11851-11858.
24. Cotter TG. Apoptosis and cancer: the genesis of a research field. Nat Rev Cancer 2009;9:501-507.

25. Weber A, Boger R, Vick B, Urbanik T, Haybaeck J, Zoller S, et al. Hepatocyte-specific deletion of the antiapoptotic protein myeloid cell leukemia-1 triggers proliferation and hepatocarcinogenesis in mice. HEPATOLOGY 2010;51:1226-1236.
26. van Delft MF, Wei AH, Mason KD, Vandenberg CJ, Chen L, Czabotar PE, et al. The BH3 mimetic ABT-737 targets selective Bcl-2 proteins and efficiently induces apoptosis via Bak/Bax if Mcl-1 is neutralized. Cancer Cell 2006;10:389-399.
27. Keuling AM, Felton KE, Parker AA, Akbari M, Andrew SE, Tron VA. RNA silencing of Mcl-1 enhances ABT-737-mediated apoptosis in melanoma: role for a caspase-8-dependent pathway. PLoS One 2009;4: e6651.
28. Yecies D, Carlson NE, Deng J, Letai A. Acquired resistance to ABT-737 in lymphoma cells that up-regulate MCL-1 and BFL-1. Blood 2010;115:3304-3313.
29. Vogler M, Dinsdale D, Sun XM, Young KW, Butterworth M, Nicotera P, et al. A novel paradigm for rapid ABT-737-induced apoptosis involving outer mitochondrial membrane rupture in primary leukemia and lymphoma cells. Cell Death Differ 2008;15:820-830.
30. Mason KD, Vandenberg CJ, Scott CL, Wei AH, Cory S, Huang DC, et al. In vivo efficacy of the Bcl-2 antagonist ABT-737 against aggressive Myc-driven lymphomas. Proc Natl Acad Sci U S A 2008;105: 17961-17966.
31. Lin X, Morgan-Lappe S, Huang X, Li L, Zakula DM, Vernetti LA, et al. 'Seed' analysis of off-target siRNAs reveals an essential role of Mcl-1 in resistance to the small-molecule Bcl-2/Bcl-XL inhibitor ABT-737. Oncogene 2007;26:3972-3979.
32. Yu C, Bruzek LM, Meng XW, Gores GJ, Carter CA, Kaufmann SH, et al. The role of Mcl-1 down-regulation in the proapoptotic activity of the multikinase inhibitor BAY 43-9006. Oncogene 2005;24: 6861-6869.
33. Ulivi P, Arienti C, Amadori D, Fabbri F, Carloni S, Tesei A, et al. Role of RAF/MEK/ERK pathway, p-STAT-3 and Mcl-1 in sorafenib activity in human pancreatic cancer cell lines. J Cell Physiol 2009;220: 214-221.
34. Blechacz BR, Smoot RL, Bronk SF, Werneburg NW, Sirica AE, Gores GJ. Sorafenib inhibits signal transducer and activator of transcription-3 signaling in cholangiocarcinoma cells by activating the phospharase shatterproof 2. HEPATOLOGY 2009;50:1861-1870.
35. Calvisi DF, Ladu S, Gorden A, Farina M, Conner EA, Lee JS, et al. Ubiquitous activation of Ras and Jak/Stat pathways in human HCC. Gastroenterology 2006;130:1117-1128.
36. Llovet JM, Ricci S, Mazzaferro V, Hilgard P, Gane E, Blanc JF, et al. Sorafenib in advanced hepatocellular carcinoma. N Engl J Med 2008; 359:378-390.
37. Cheng AL, Kang YK, Chen Z, Tsao CJ, Qin S, Kim JS, et al. Efficacy and safety of sorafenib in patients in the Asia-Pacific region with advanced hepatocellular carcinoma: a phase III randomised, double-blind, placebo-controlled trial. Lancet Oncol 2009;10:25-34.